"Novel rheological characterization platforms for the extrudability and safety analysis of energetic materials "

Joint Ordnance Commanders Group (JOCG)
Continuous Mixer & Extruder Users Group (CMEUG)

13-14 October 2004

Dilhan M. Kalyon, Halil Gevgilili, Elvan Birinci, Hansong Tang
Stevens Institute of Technology, Castle Point
Hoboken, NJ 07030
and
James Kowalczyk and Bahadir Karuv
Material Processing & Research, Inc.
31 Mercer St. 2-E, Hackensack, NJ 07661

Figure 1

Why is the rheological characterization of highly filled materials such a challenge?

Figure 2

Demonstration of Apparent Wall Slip

60% vol. solids

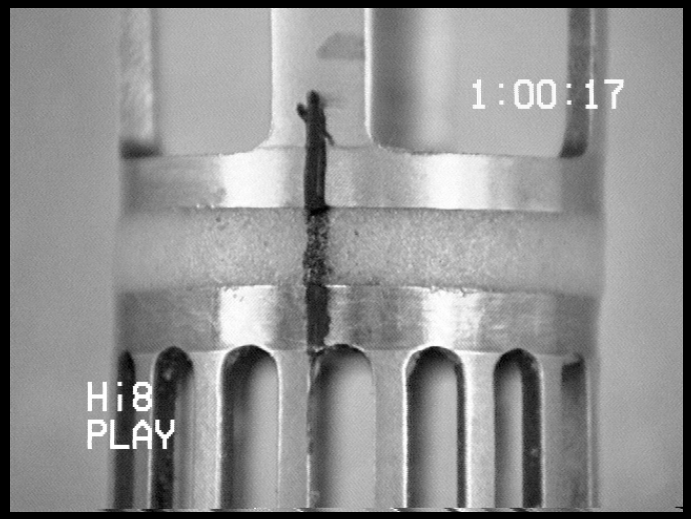

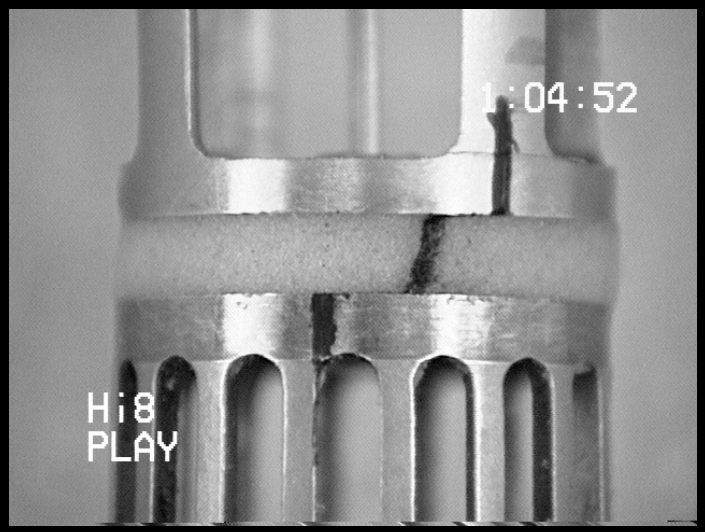

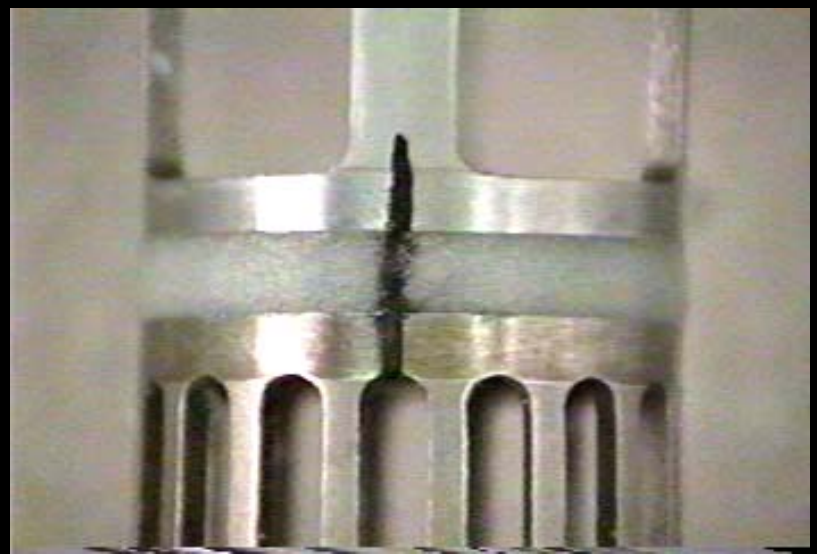

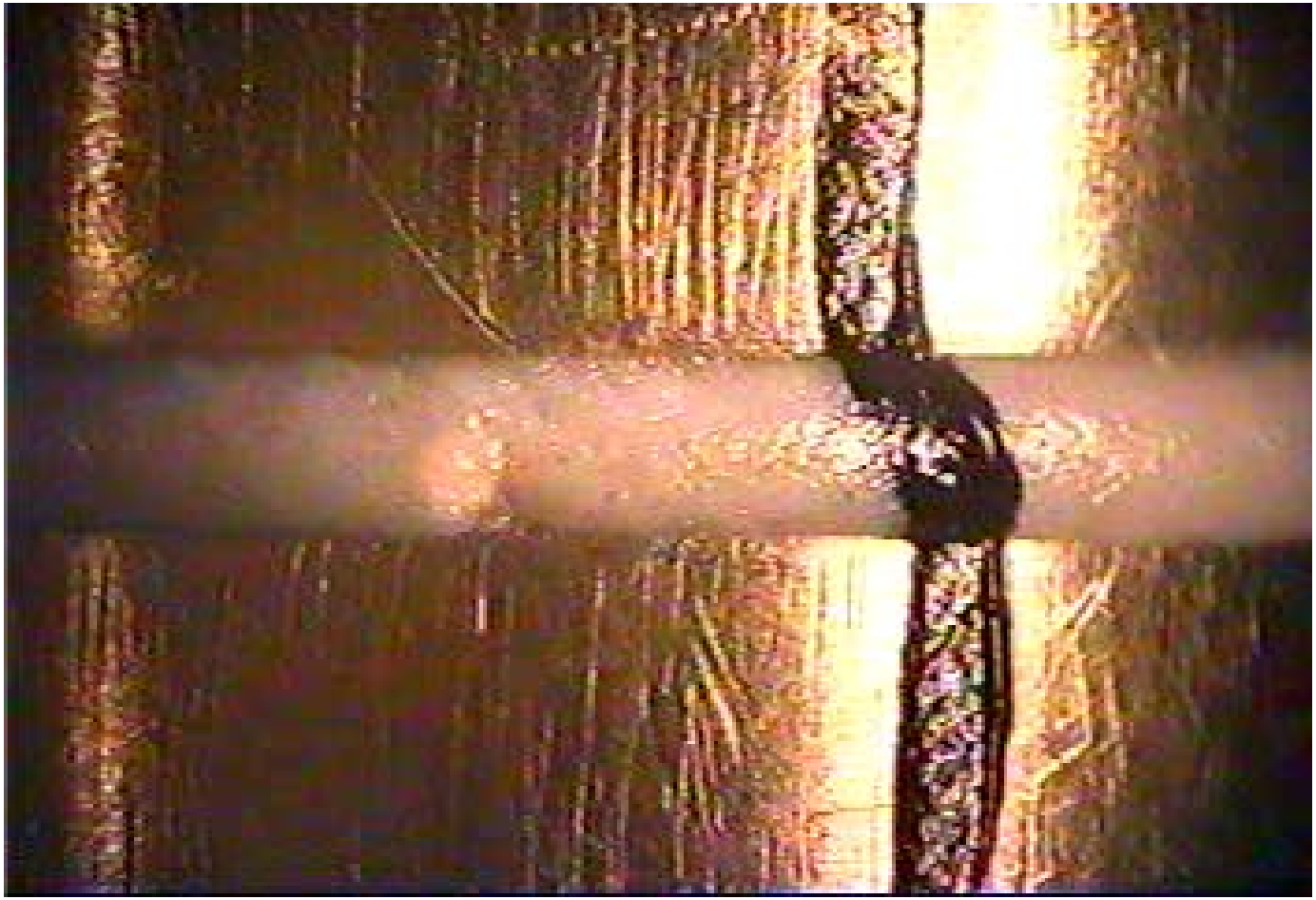

Small amplitude oscillatory shear: strain sweep with a concentrated suspension

Figure 4

Demonstration of Viscoplasticity

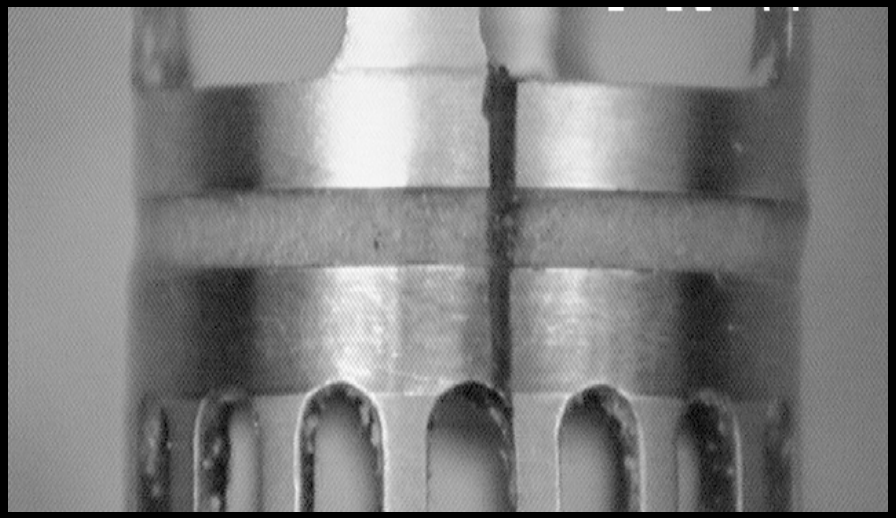

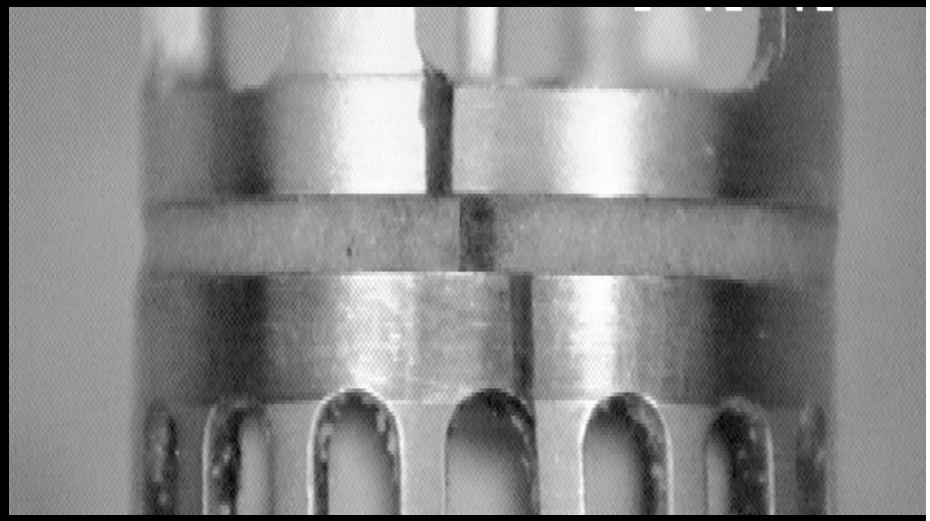

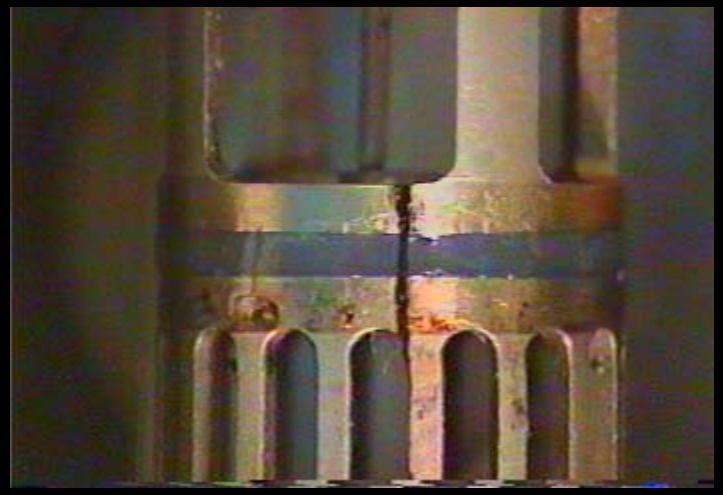

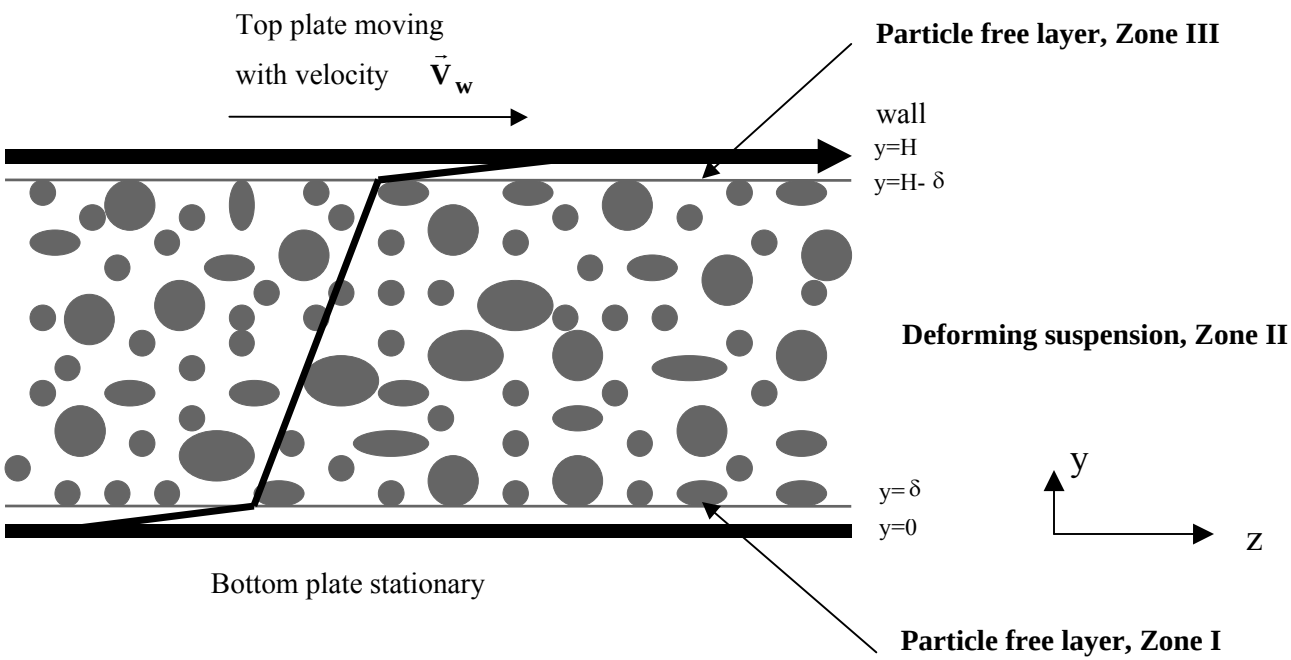
Top plate moving
with velocity $\vec{V}_w$
Particle free layer, Zone III
wall
y=H
y=H- δ
Deforming suspension, Zone II
y= δ
y=0
y
z
Bottom plate stationary
Particle free layer, Zone I

Figure 6

Suspension:

$$\tau_{yz} = \pm\tau_0 - m\left|\frac{dV_z}{dy}\right|^{n-1}\left(\frac{dV_z}{dy}\right)$$

Binder:

$$\tau_{yz} = -m_b\left|\frac{dV_z}{dy}\right|^{n_b-1}\left(\frac{dV_z}{dy}\right)$$

Figure 7

$$V_z^{I} = \left(\frac{-\tau_{yz}}{m_b} \right)^{s_b} y \qquad \text{for } 0 \le y \le \delta$$

$$V_z^{II} = \delta \left(\frac{-\tau_{yz}}{m_b} \right)^{s_b} + \left(\frac{-(\tau_{yz} + \tau_0)}{m} \right)^{s} (y - \delta) \qquad \text{for } \delta \le y \le (H - \delta)$$

$$V_z^{III} = \overline{V}_W + \left(\frac{-\tau_{yz}}{m_b} \right)^{s_b} (y - H) \qquad \text{for } (H - \delta) \le y \le H$$

Figure 8

$$\left(\frac{-(\tau_{yz}+\tau_0)}{m}\right)^{s}(1-2\delta^{*})+2\delta^{*}\left(\frac{-\tau_{yz}}{m_b}\right)^{s_b}=\frac{\overline{V}_w}{H}$$

$$\left.\frac{\partial\left(\overline{V}_w/H\right)}{\partial(1/H)}\right|_{\tau_{yz}}=2\delta\left(\frac{-\tau_{yz}}{m_b}\right)^{s_b}-2\delta\left(\frac{-(\tau_{yz}+\tau_0)}{m}\right)^{s}\cong 2\,V_z^{\,I}\Big|_{y=\delta}=2\;U_s\Big|_{y=\delta}$$

Determination of slip velocity, Us for plane Couette flow
Steady torsional and cone-and-plate flows

Figure 9

True shear rate at the wall:

$$\frac{dV_z^{II}}{dy} = \frac{\overline{V}_w - 2U_s\left(\tau_{yz}\right)}{H - 2\delta}$$

$$U_s = \pm\beta\left(-\tau_{yz}\right)^{s_b} = \pm\frac{\delta}{m_b^{\,s_b}}\left(-\tau_{yz}\right)^{s_b}$$

Slip velocity versus the shear stress relationship

Figure 10

$$\beta = \frac{\delta}{m_b^{s_b}}$$

Navier's slip coefficient is related to the slip layer thickness
And also the parameters of the shear viscosity of the binder.

Figure 11

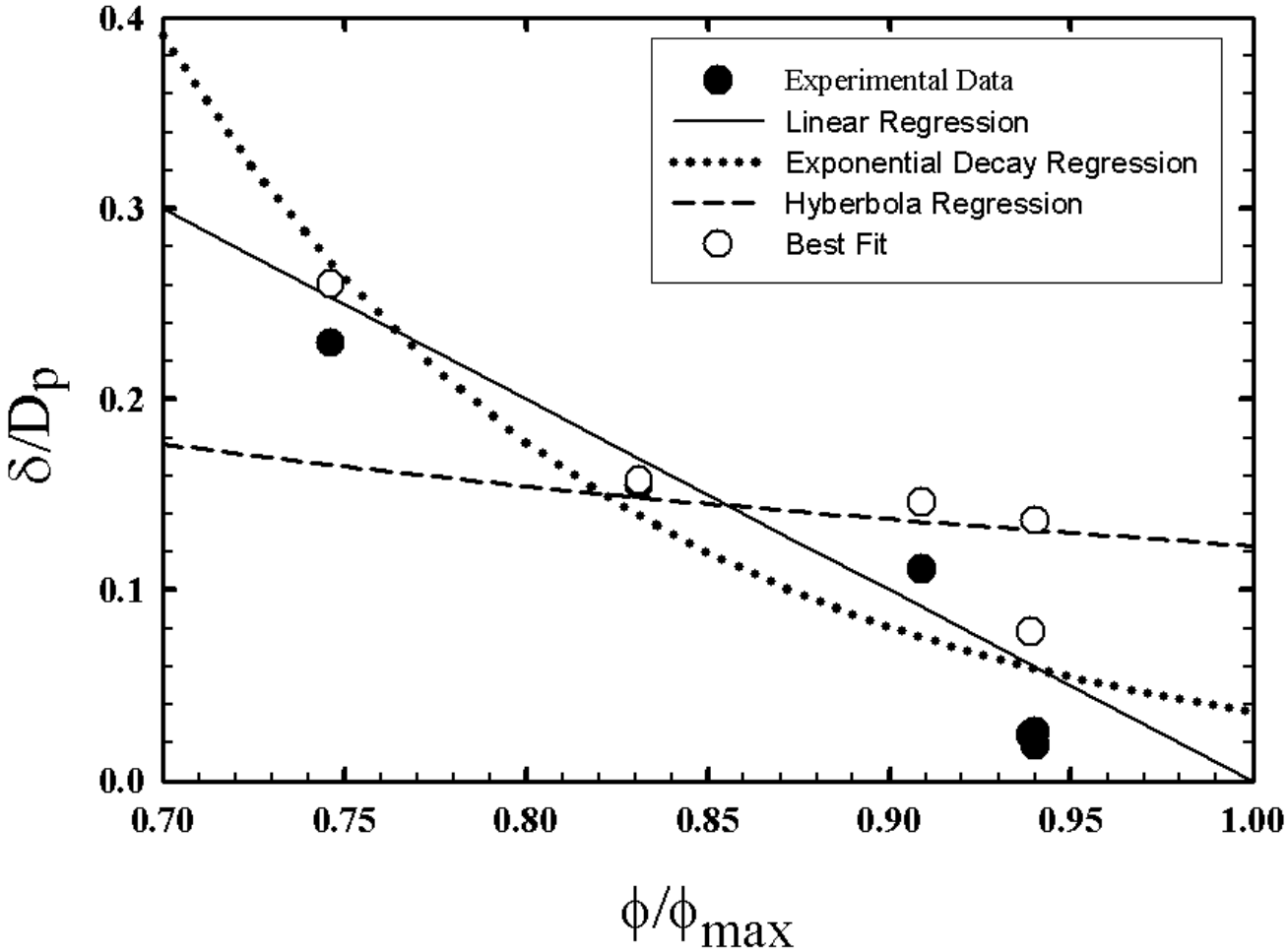

Linear

$$\frac{\delta}{D_p} = 1 - \frac{\phi}{\phi_m}$$

Exponential

$$\frac{\delta}{D_p} = \left(100 \times e^{-8*\frac{\phi}{\phi m}}\right)$$

Hyperbolic

$$\frac{\delta}{D_p} = \frac{100}{1 + \frac{1}{.0012}\frac{\phi}{\phi m}}$$

Figure 12

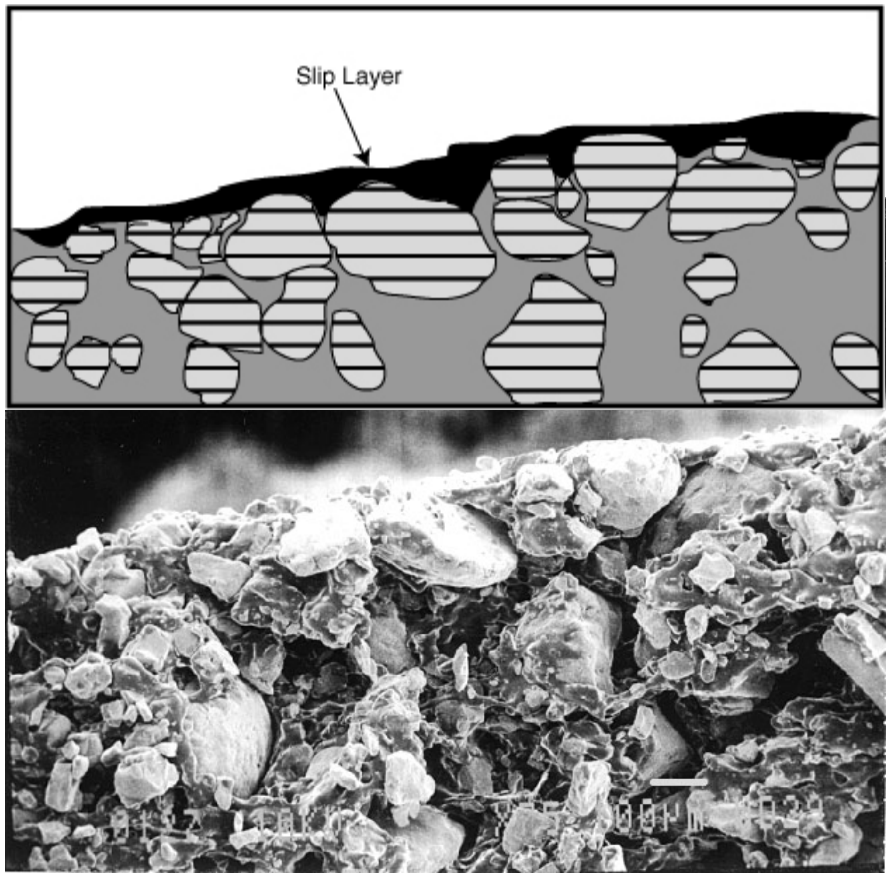

Figure 13

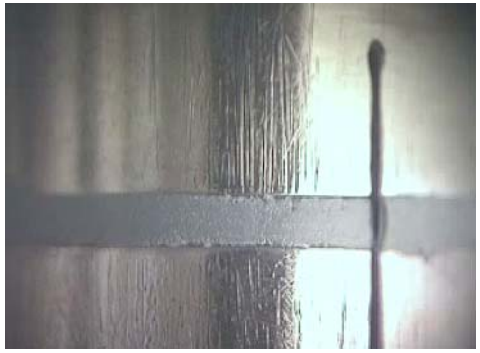

a

b. Deforming suspension with wall slip

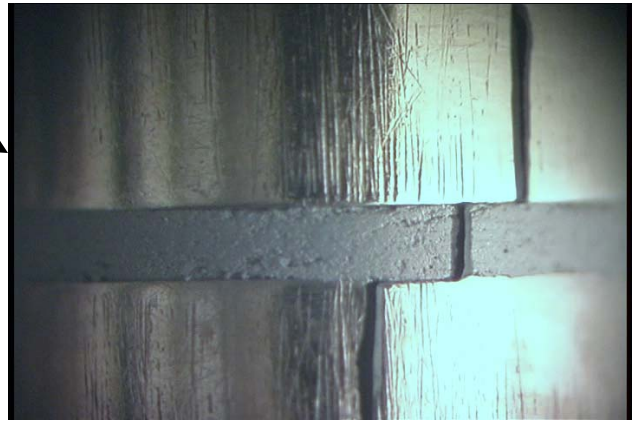

c. Plug flow

Figure 14

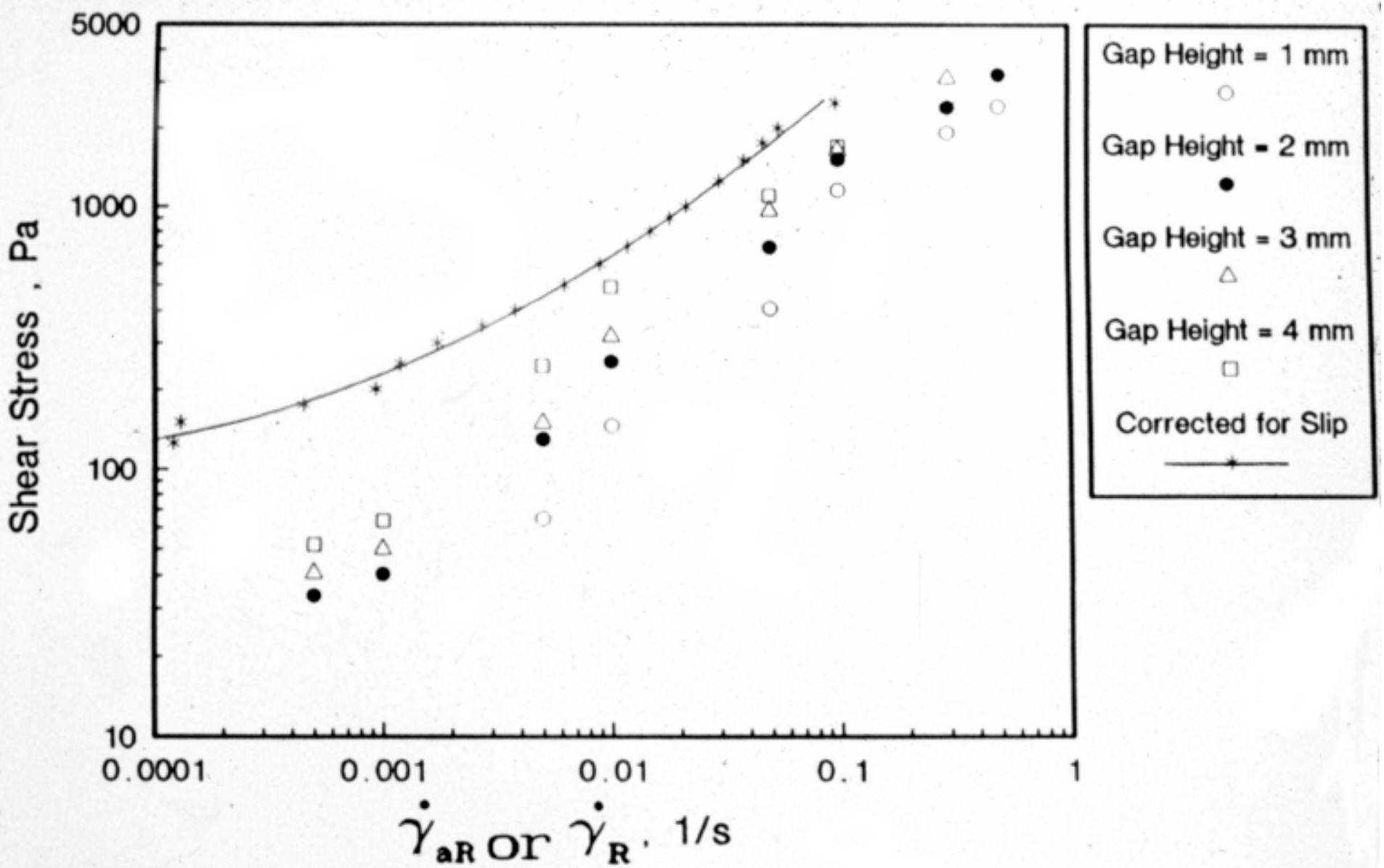

Figure 8

Figure 15

disk torsional flow of suspension 1.

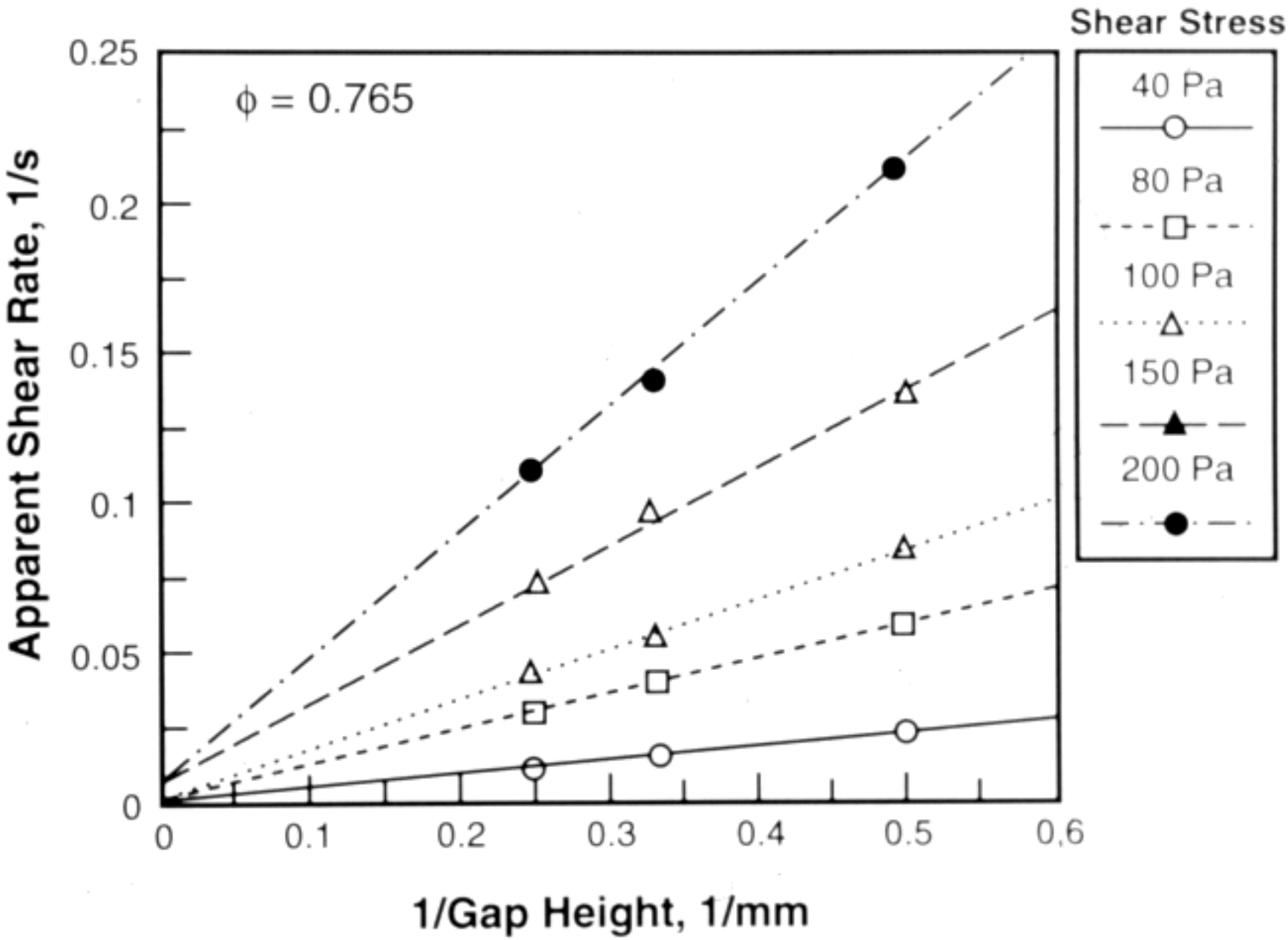

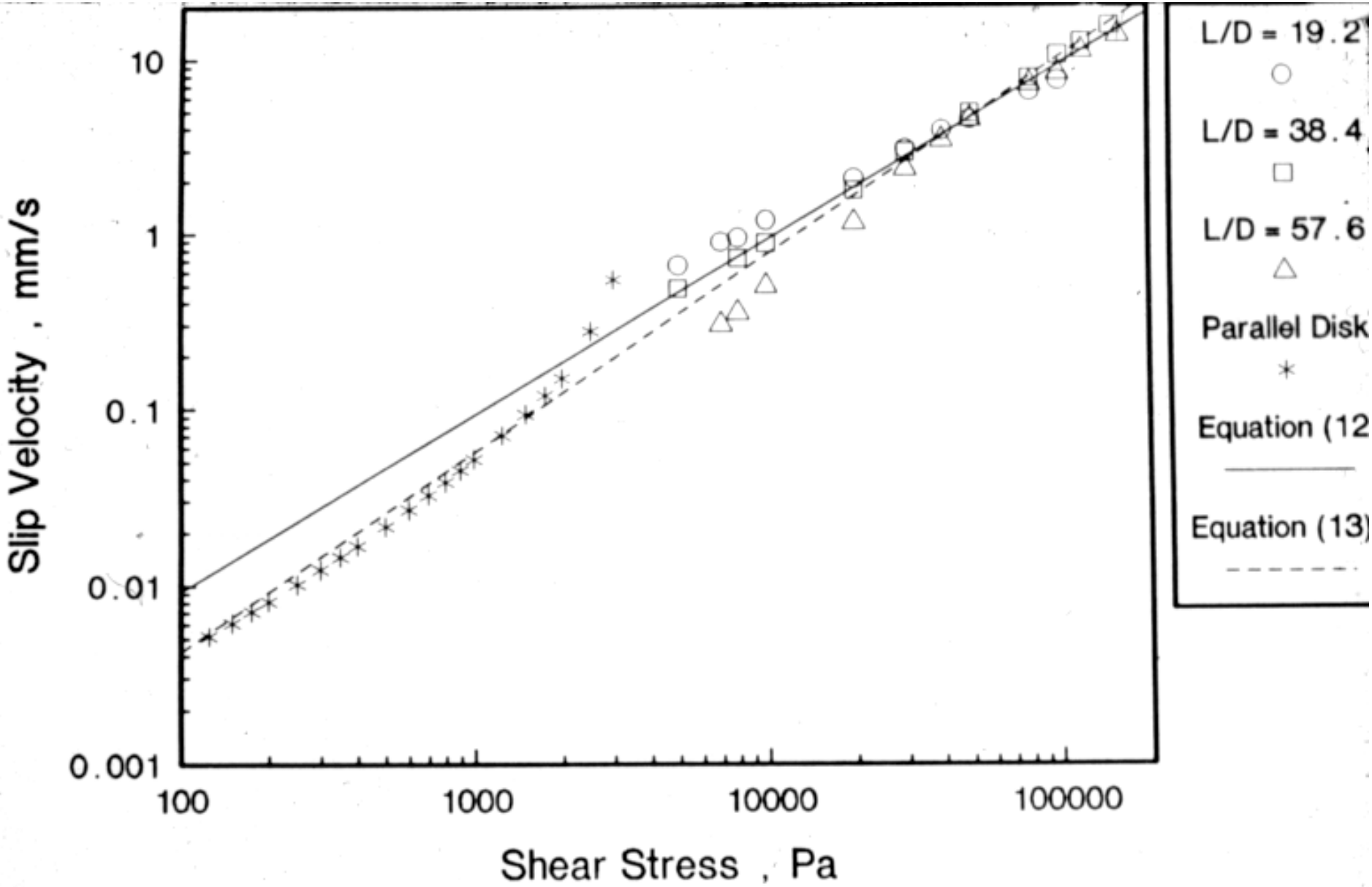

Figure 5

Figure 17

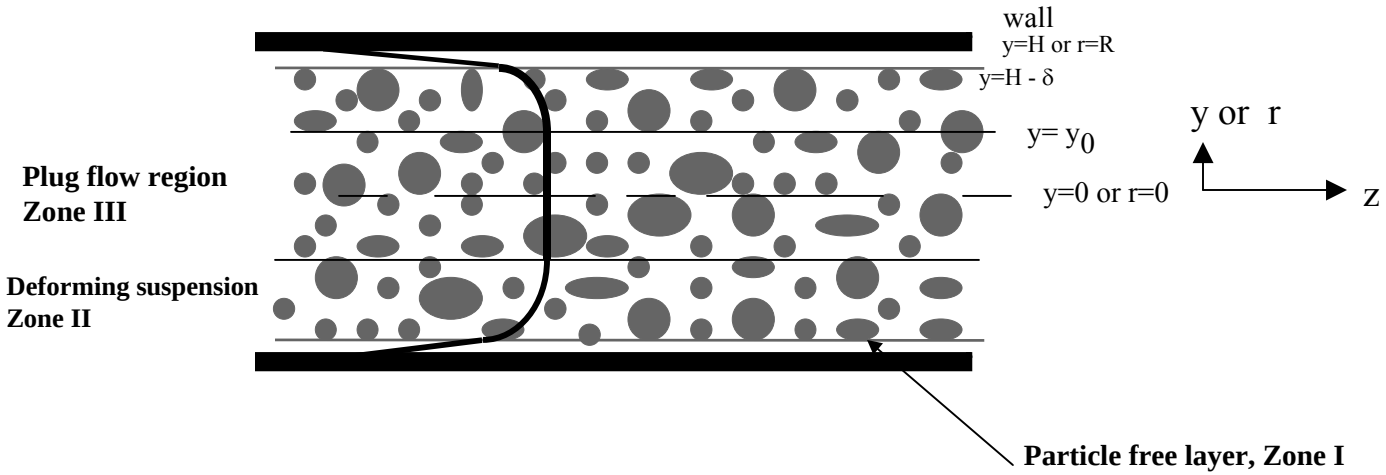

Flow in a tube die: Capillary flow

Figure 18

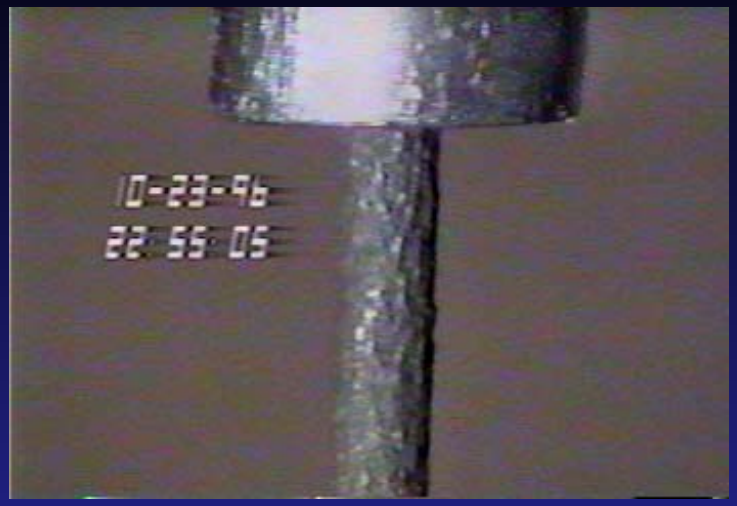

Extrudate with 76.5% solids prior to axial migration of binder

Unstable flow

Filtration of the binder phase

Figure 19

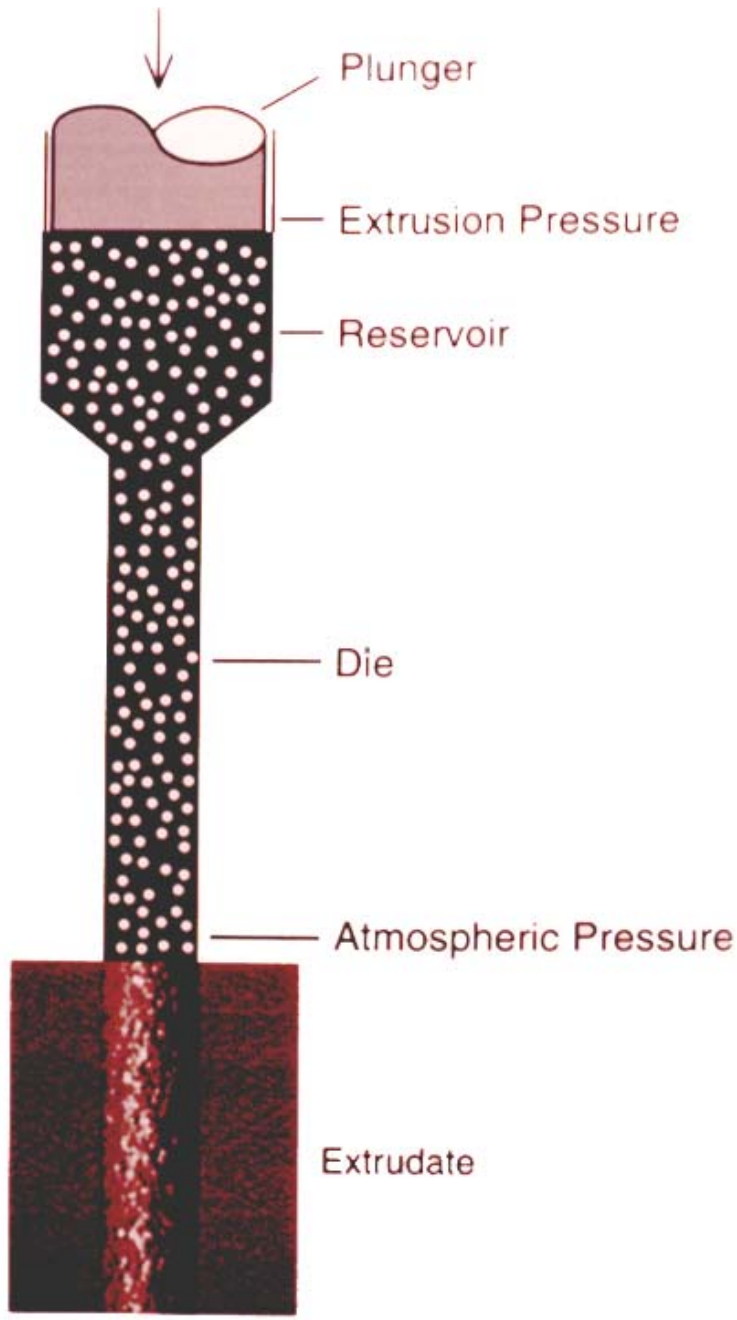
Plunger
Extrusion Pressure
Reservoir
Die
Atmospheric Pressure
Extrudate

Figure 20

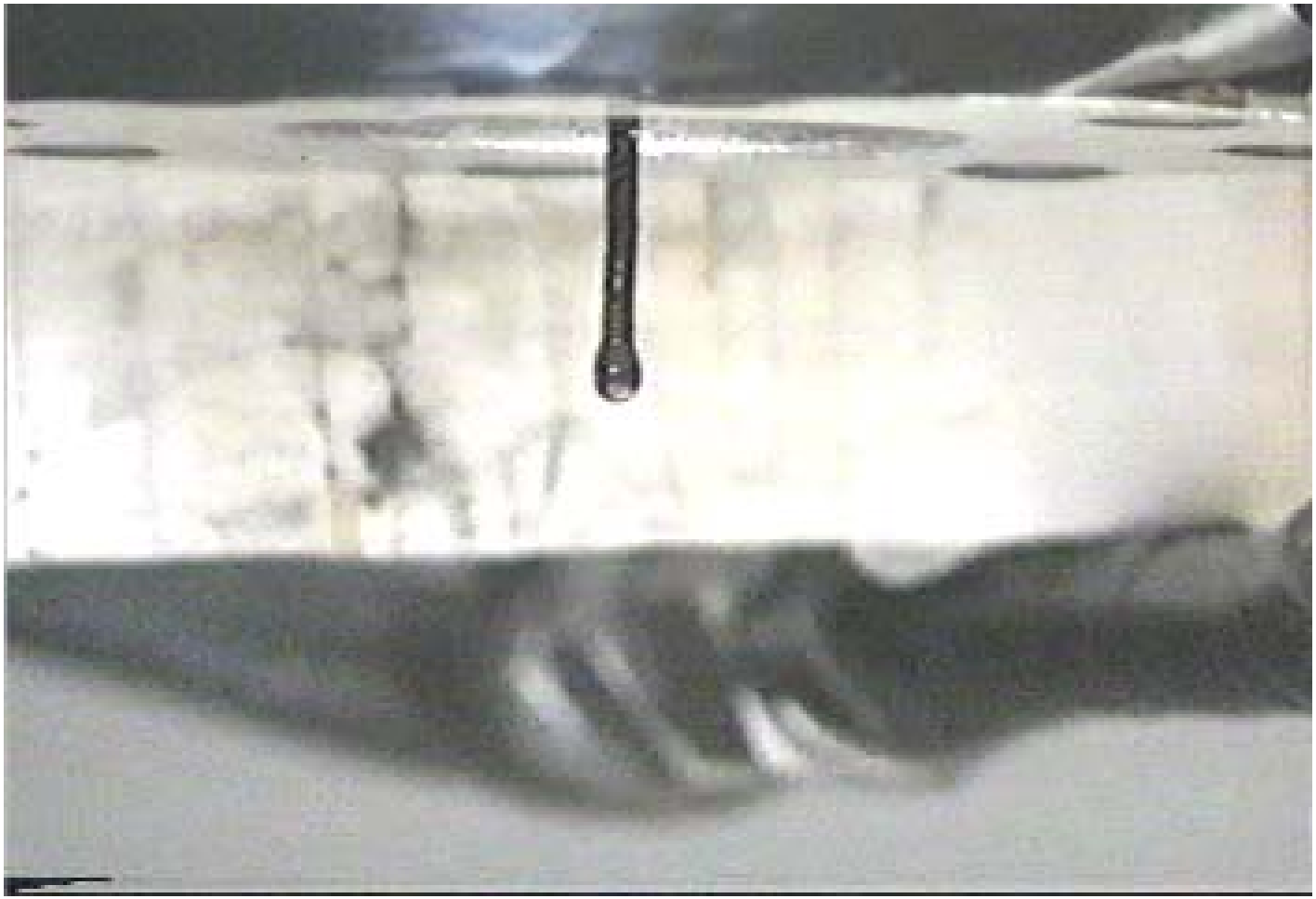

Segregation of the binder for a battery suspension

Figure 21

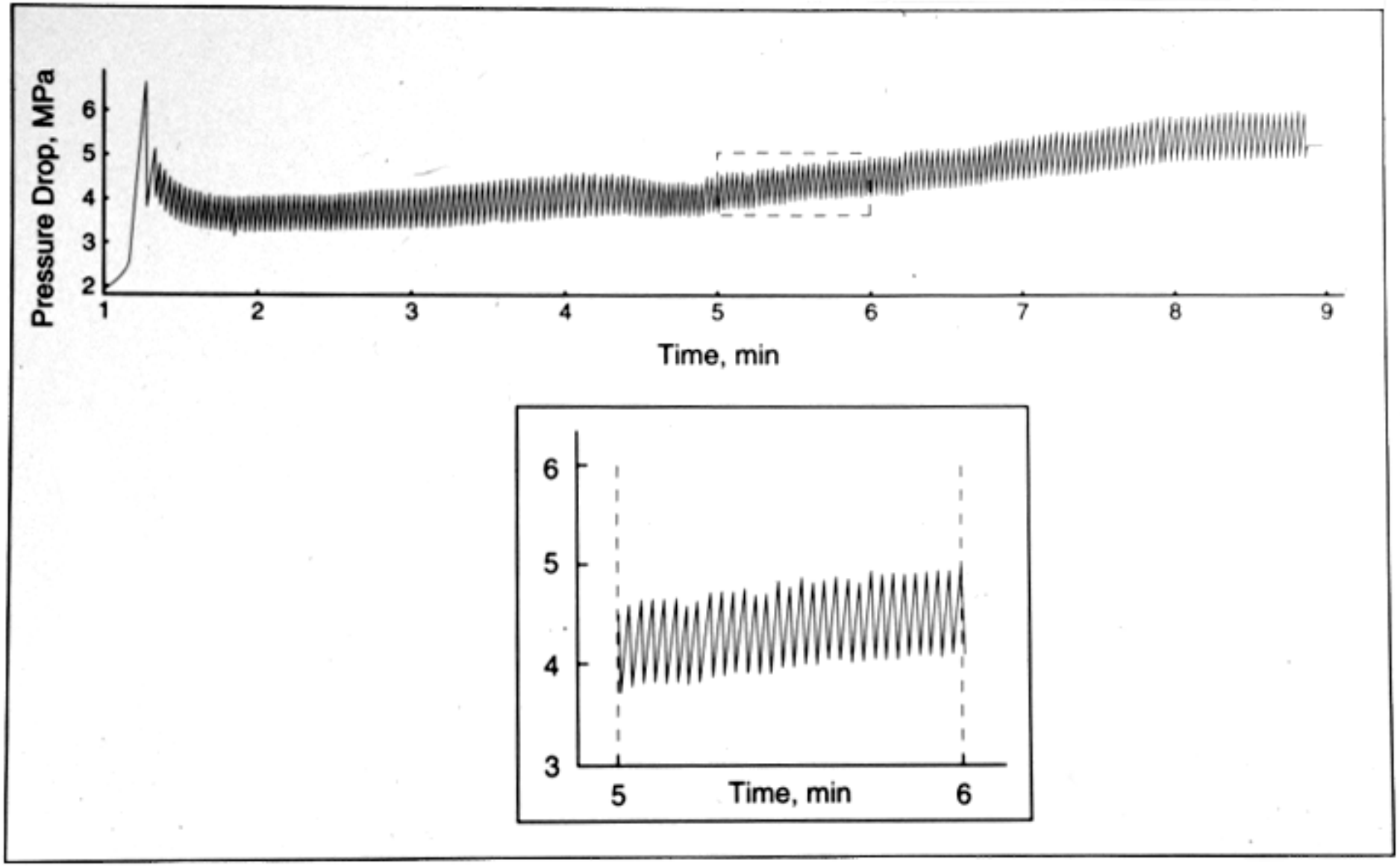

Figure 22

Development of Concentration Profile in the Reservoir during Capillary Flow upon Axial Migration of the Polymer

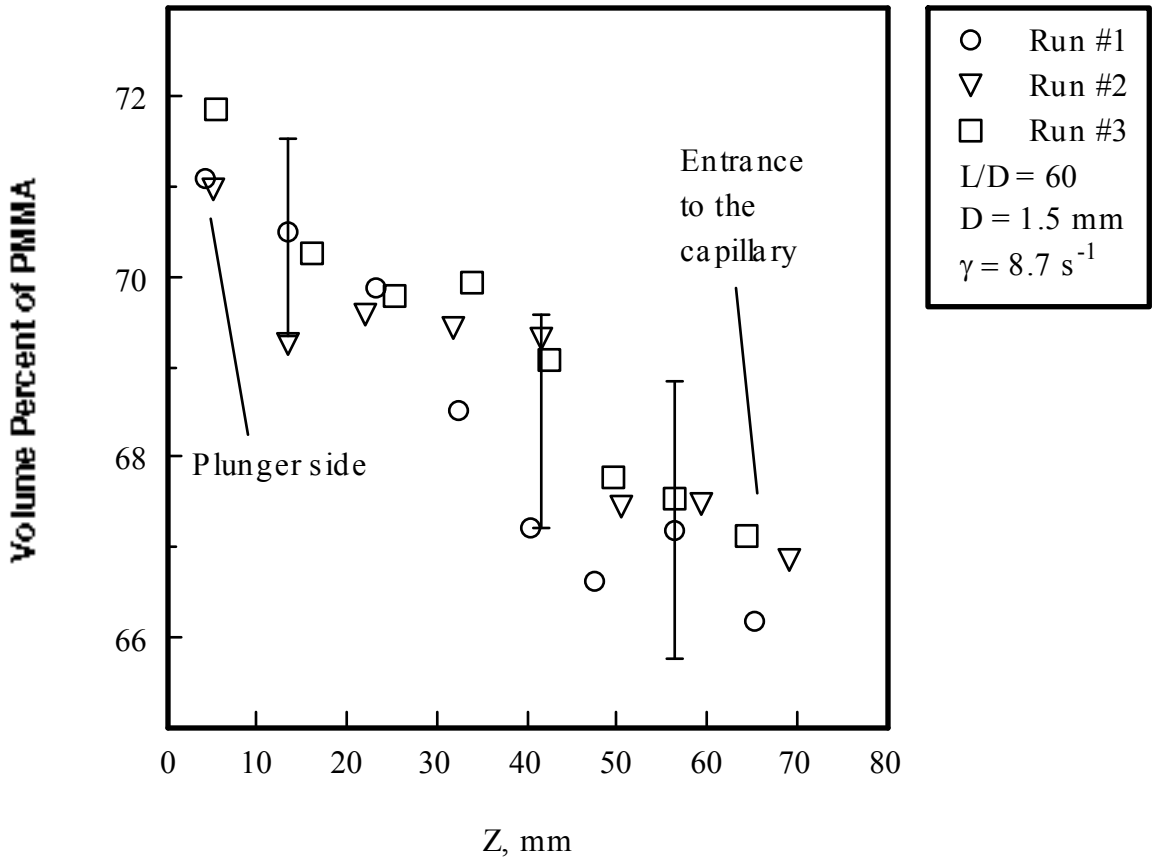

Figure 23

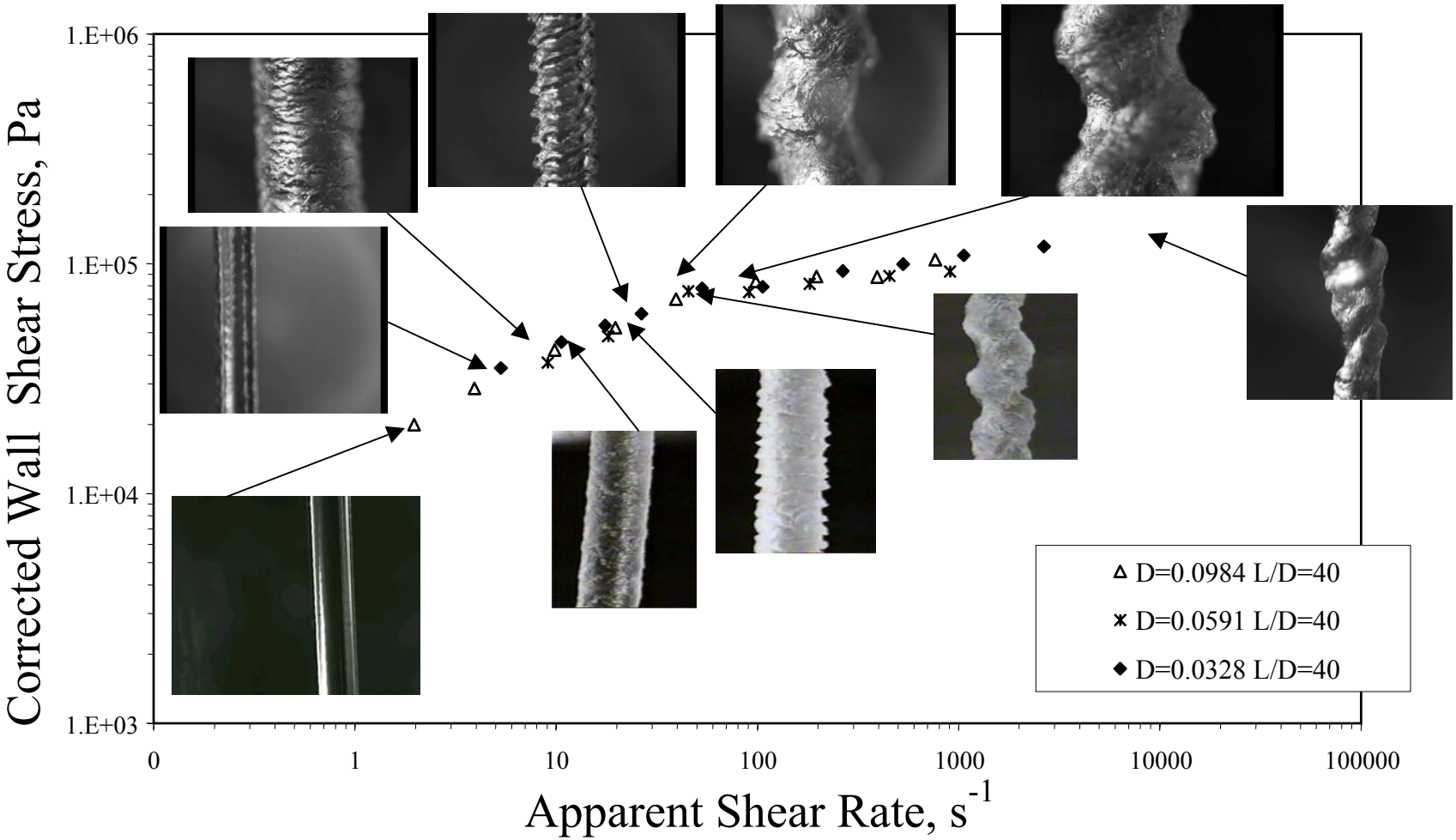

Fig. 2. Flow curves and extrudates of poly(dimethyl siloxane) collected with capillaries with different diameters and development of extrudate surface irregularities

Figure 24

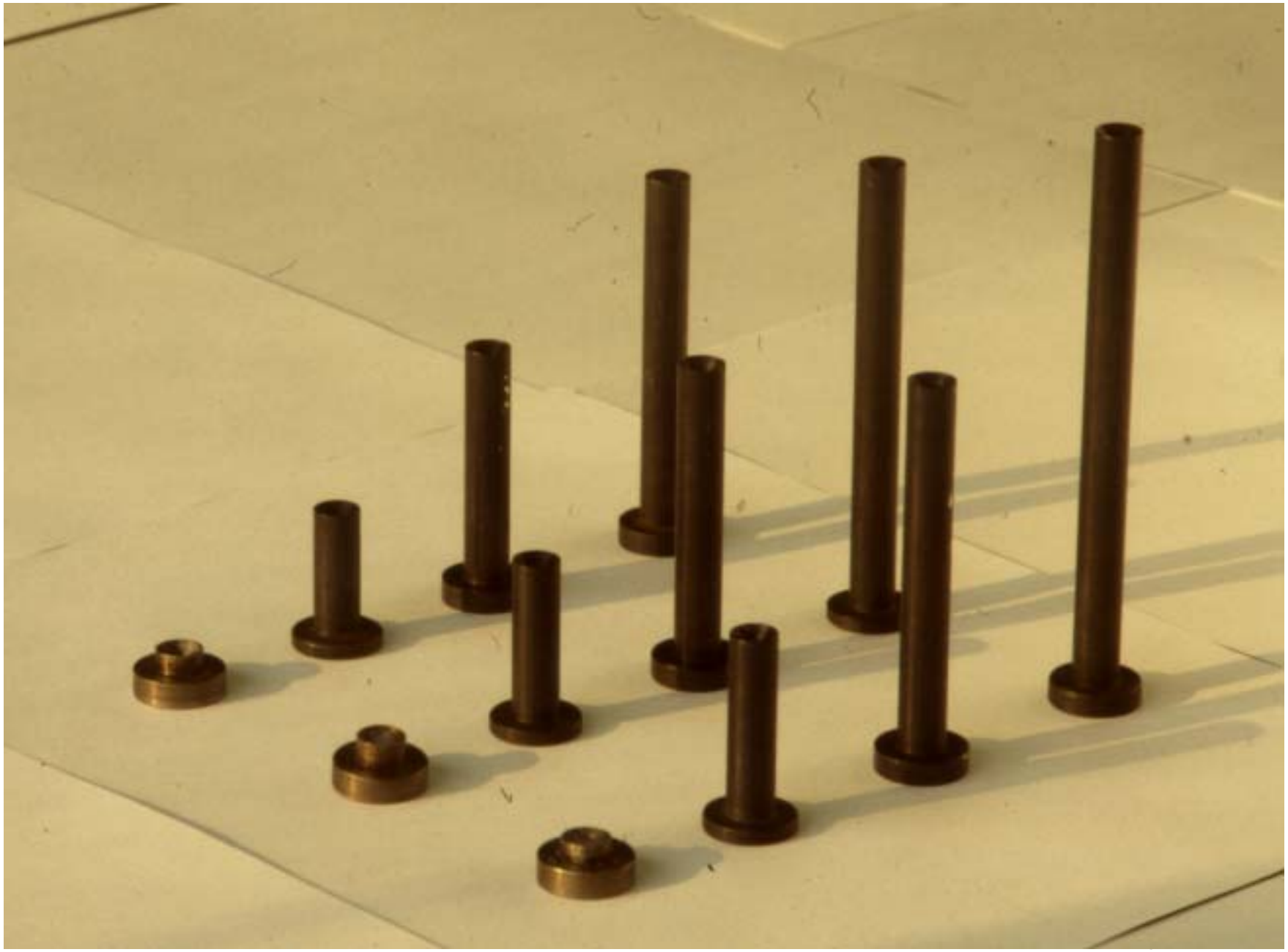

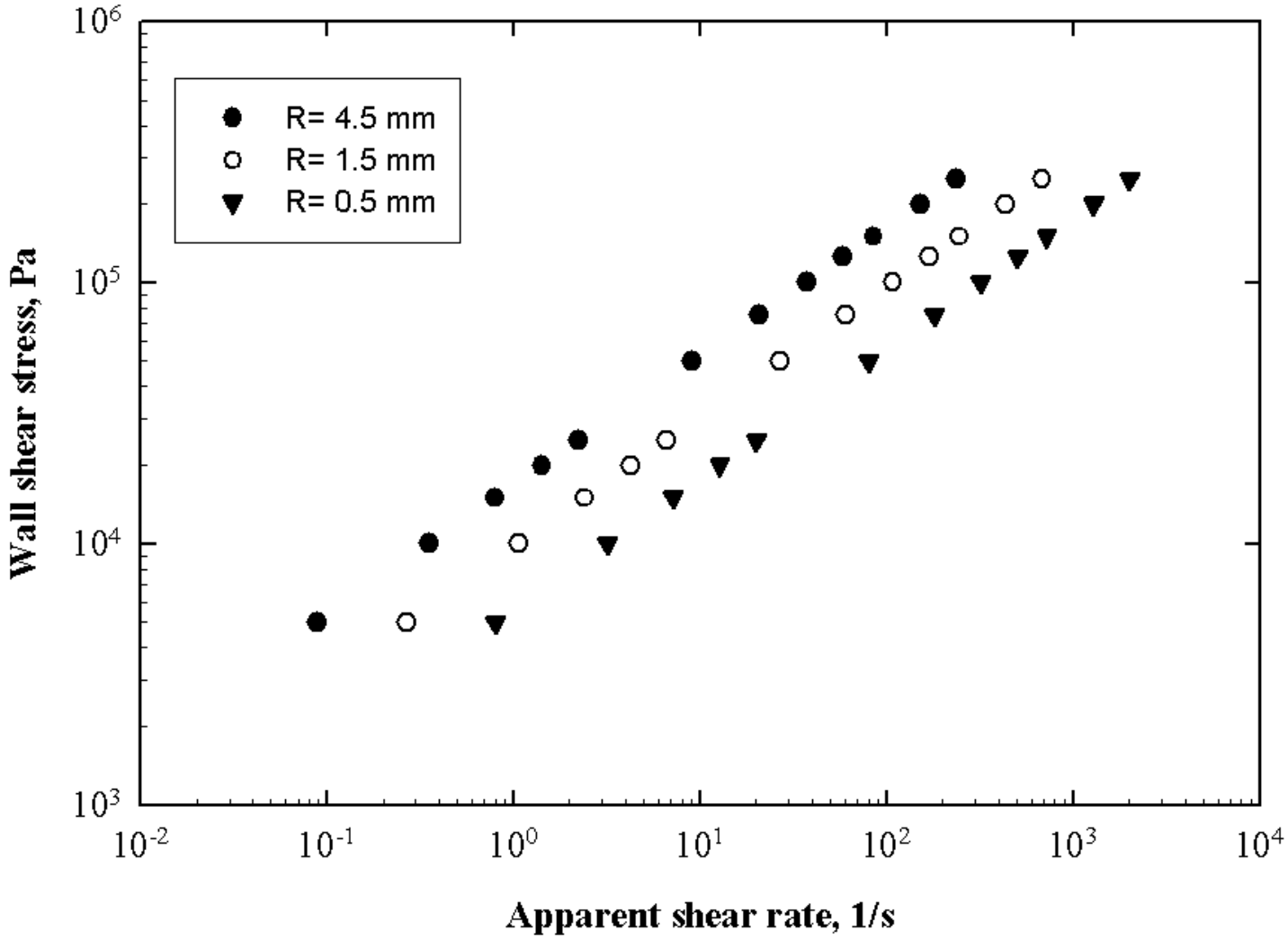
R= 4.5 mm
R= 1.5 mm
R= 0.5 mm
Wall shear stress, Pa
Apparent shear rate, 1/s
10^6
10^5
10^4
10^3
10^{-2}
10^{-1}
10^0
10^1
10^2
10^3
10^4

Figure 26

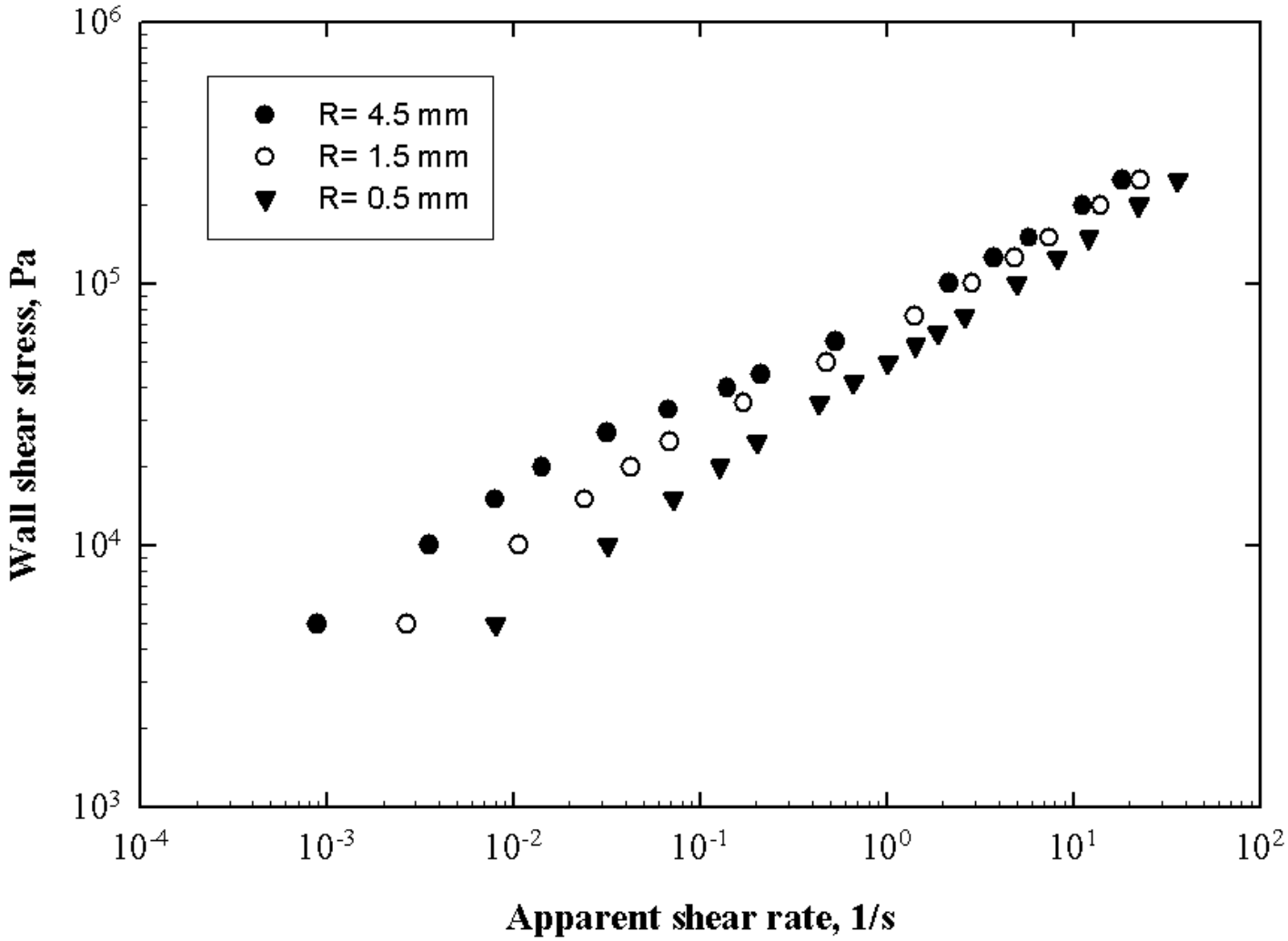
R= 4.5 mm
R= 1.5 mm
R= 0.5 mm
Wall shear stress, Pa
Apparent shear rate, 1/s
10^6
10^5
10^4
10^3
10^{-4}
10^{-3}
10^{-2}
10^{-1}
10^0
10^1
10^2

Figure 27

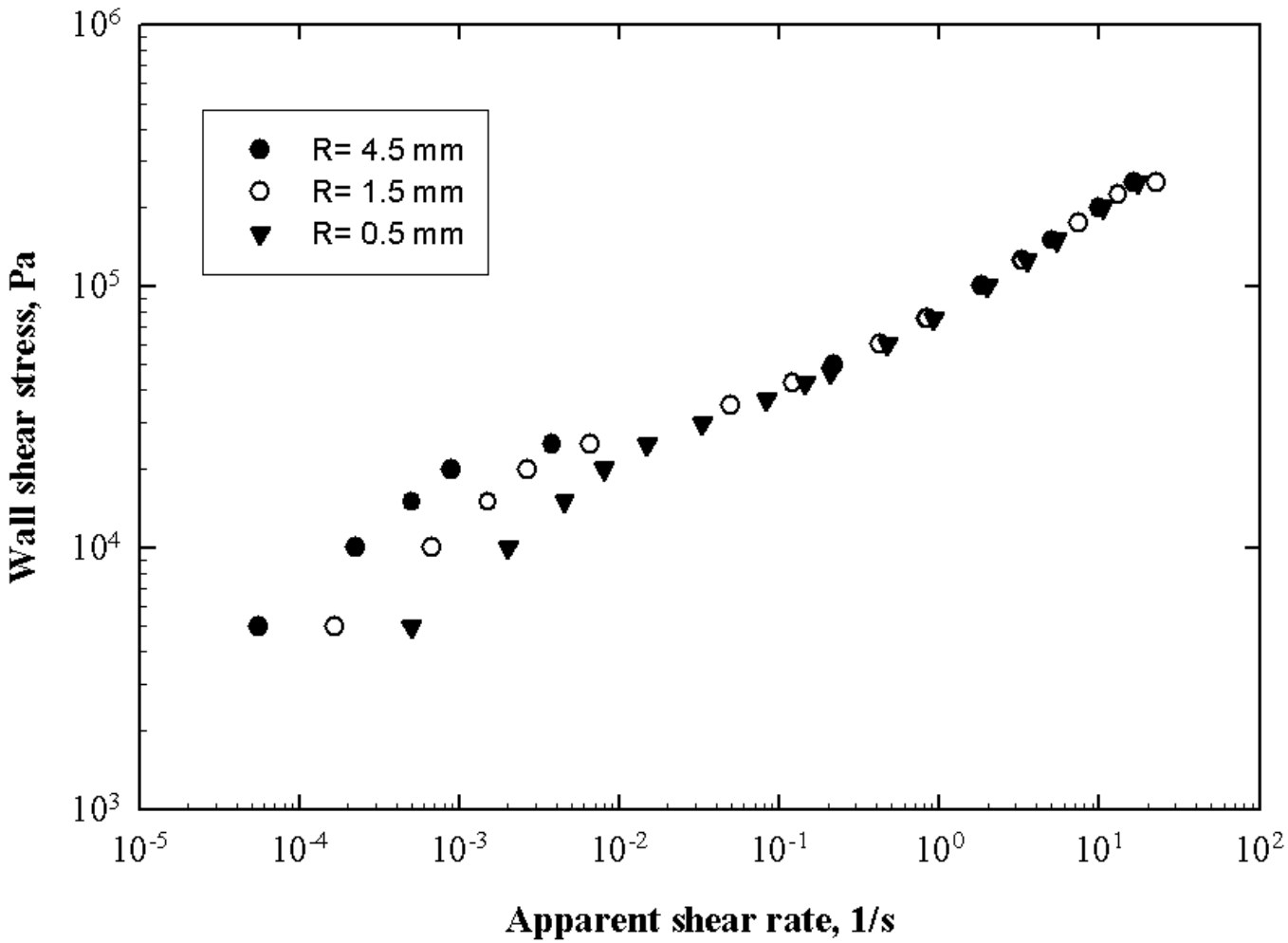
R= 4.5 mm
R= 1.5 mm
R= 0.5 mm
Wall shear stress, Pa
Apparent shear rate, 1/s
10^6
10^5
10^4
10^3
10^{-5}
10^{-4}
10^{-3}
10^{-2}
10^{-1}
10^0
10^1
10^2

Figure 28

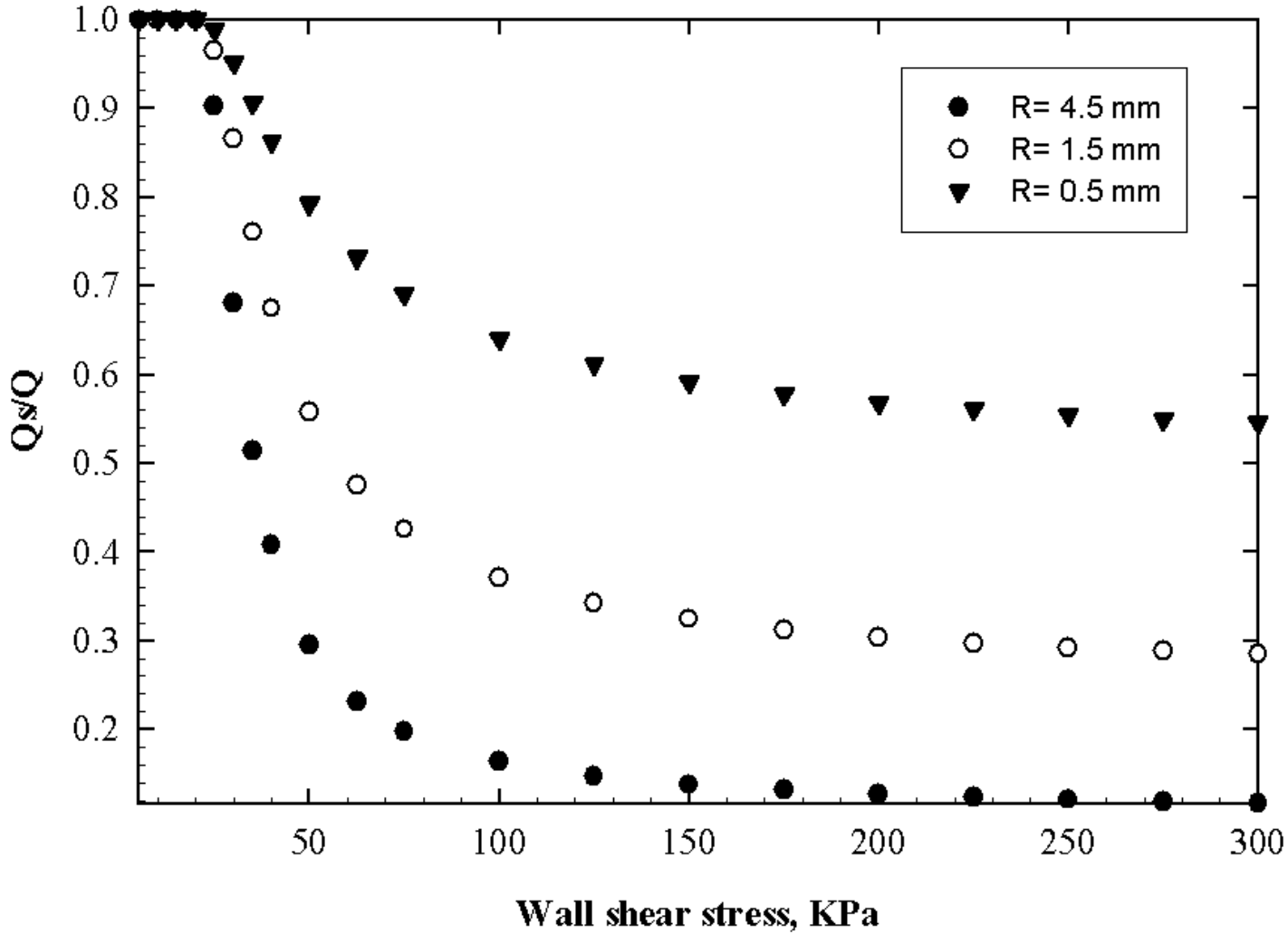
1.0
0.9
0.8
0.7
0.6
0.5
0.4
0.3
0.2
Qs/Q
50
100
150
200
250
300
Wall shear stress, KPa
R= 4.5 mm
R= 1.5 mm
R= 0.5 mm

Figure 29

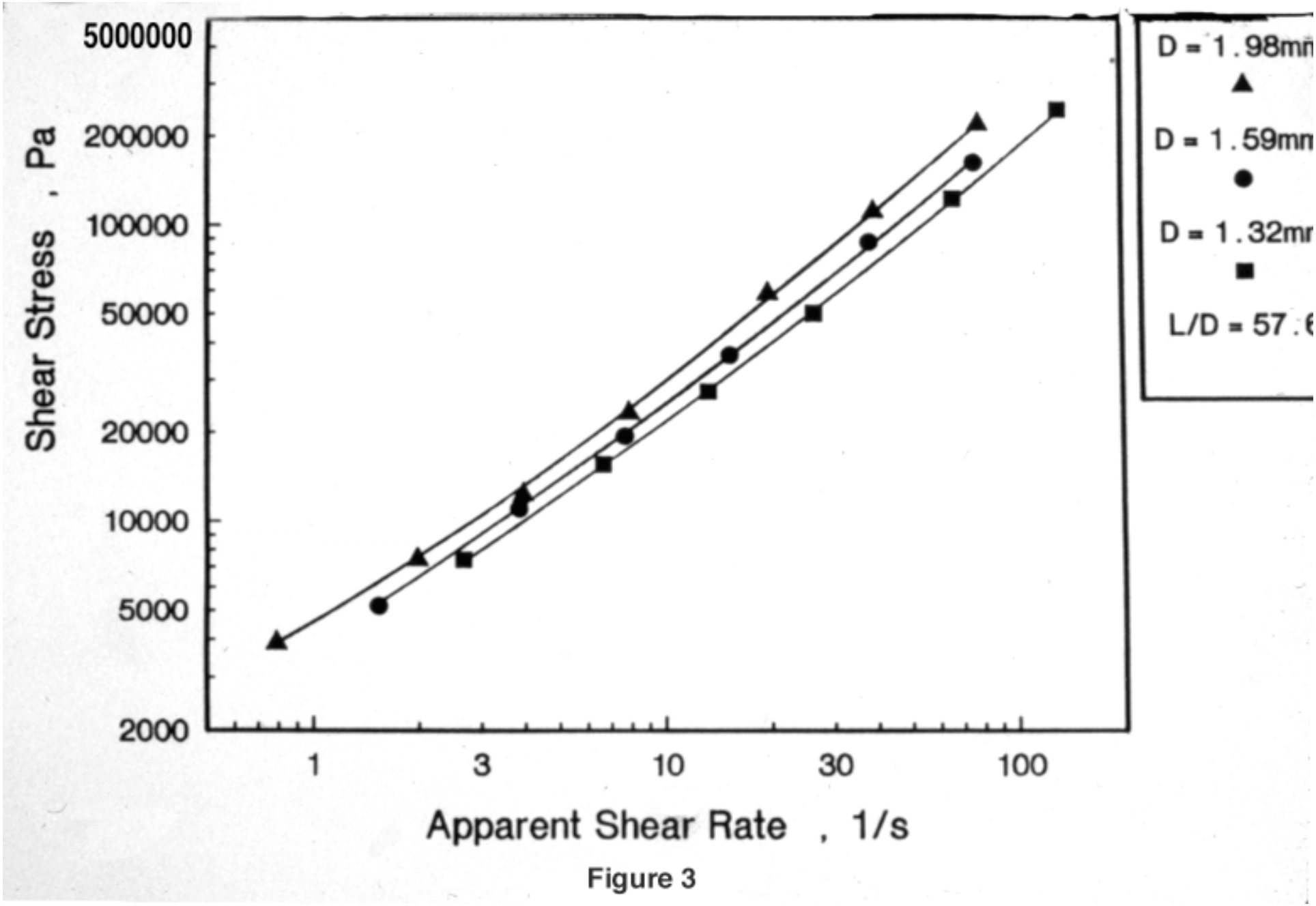
5000000
200000
100000
50000
20000
10000
5000
2000
Shear Stress , Pa
1
3
10
30
100
Apparent Shear Rate , 1/s
D = 1.98mm
D = 1.59mm
D = 1.32mm
L/D = 57.6
Figure 3

Figure 30

Viscoplastic fluids

a) for analytical solutions

$$\tau_{yz} = -m\left|\frac{du_z}{dy}\right|^{n-1}\frac{du_z}{dy} \pm \tau_0$$

$$\frac{du_z}{dy} = 0 \qquad\qquad \left|\tau_{yz}\right| \le \tau_0$$

b) for numerical solutions, 2-D and 3-D FEM, Papanastasiou Eq'n:

$$\eta = \left[m_0(|\dot{\gamma}|)^{n-1} + \frac{\tau_o(1-\exp(-n_b|\dot{\gamma}|))}{|\dot{\gamma}|}\right]\exp(-c'(T-T_0))$$

Figure 31

Uniaxial extensional rheometer

Figure 32

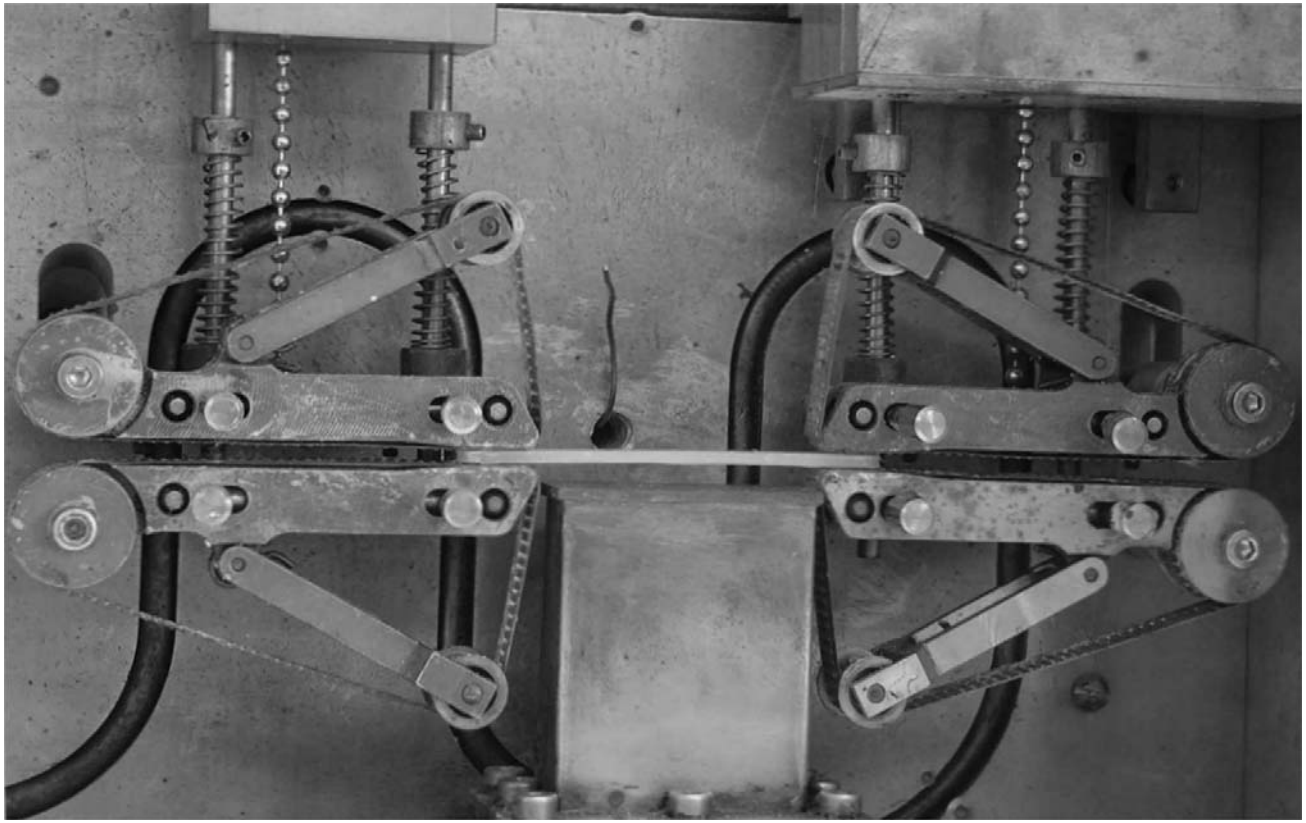

Rotary clamp system of the rheometer

Figure 33

Figure 34

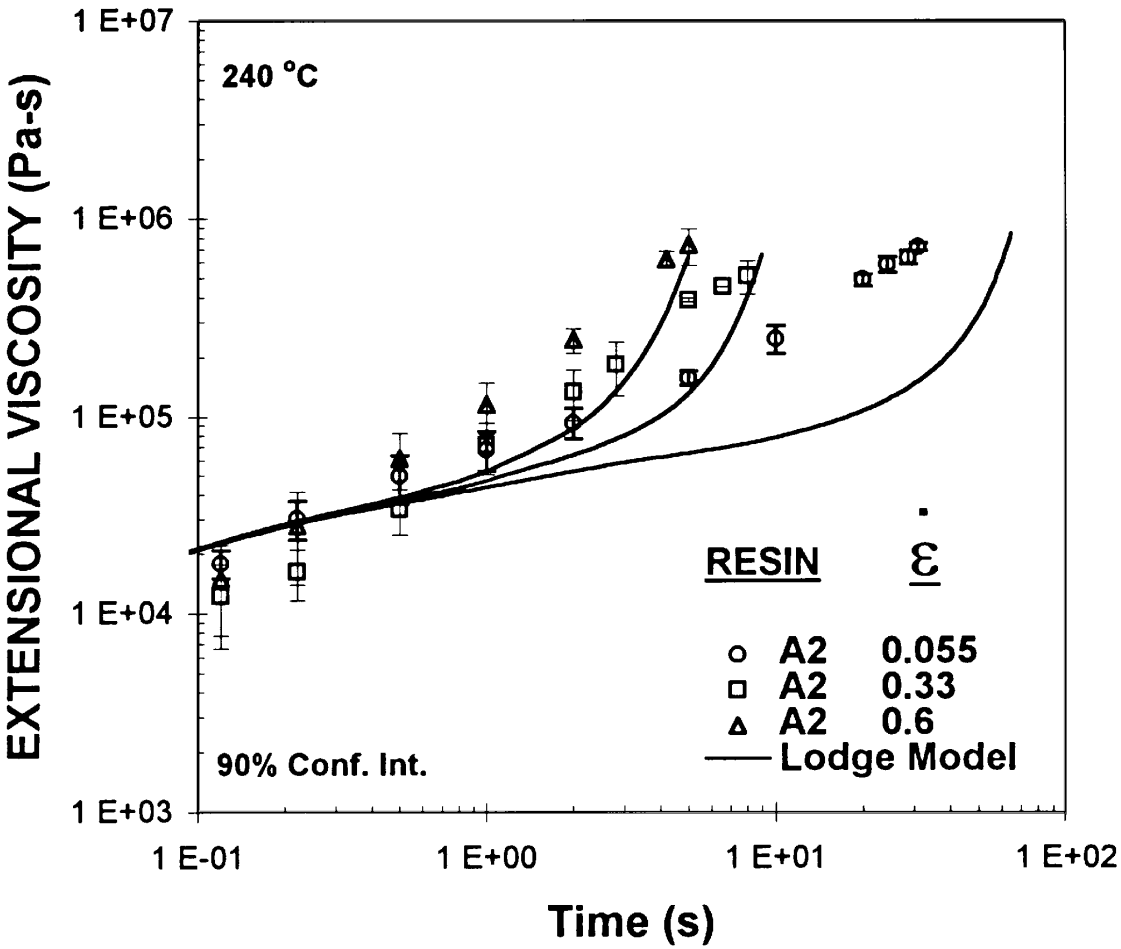

Extensional stress growth vs. time behavior of glass filled polyamide 6 at three strain rates and comparisons with predictions of Lodge model.

Figure 35

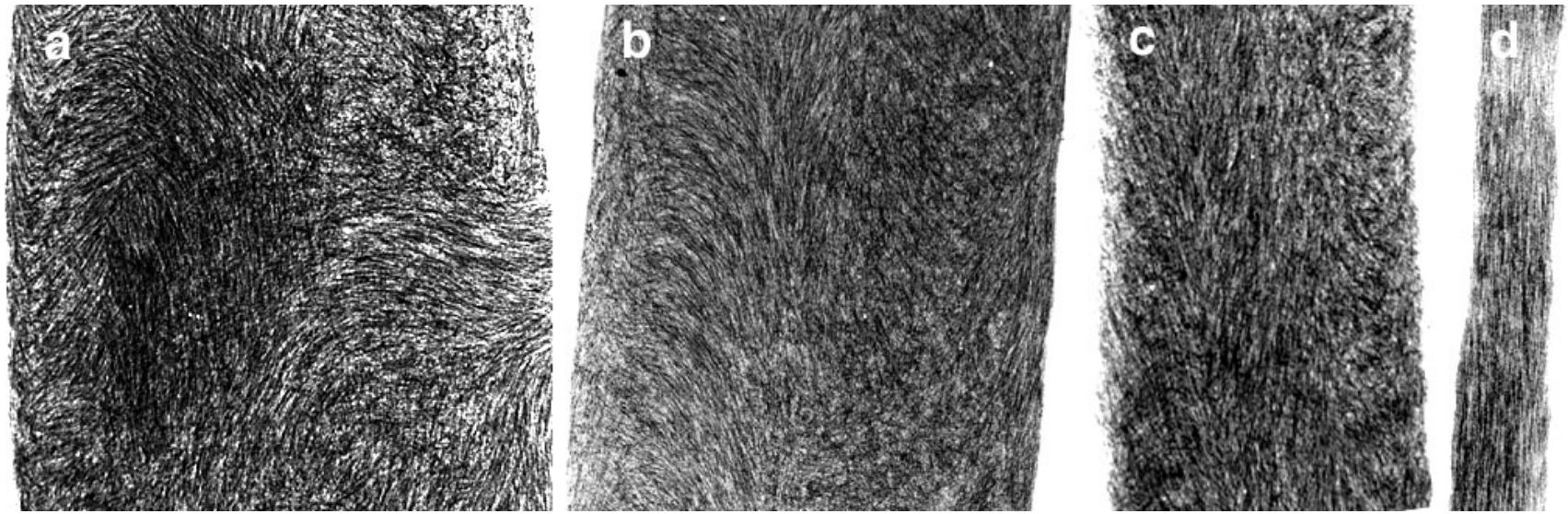

a) ε=0, J=0.16 **b) ε =.55, J=0.40** **c) ε =1.1 J=0.61** **d) ε =2.75 J= .84**

Microradiographs (5X) of extensional samples subject to various strains, ε and the corresponding fiber orientation

Figure 36

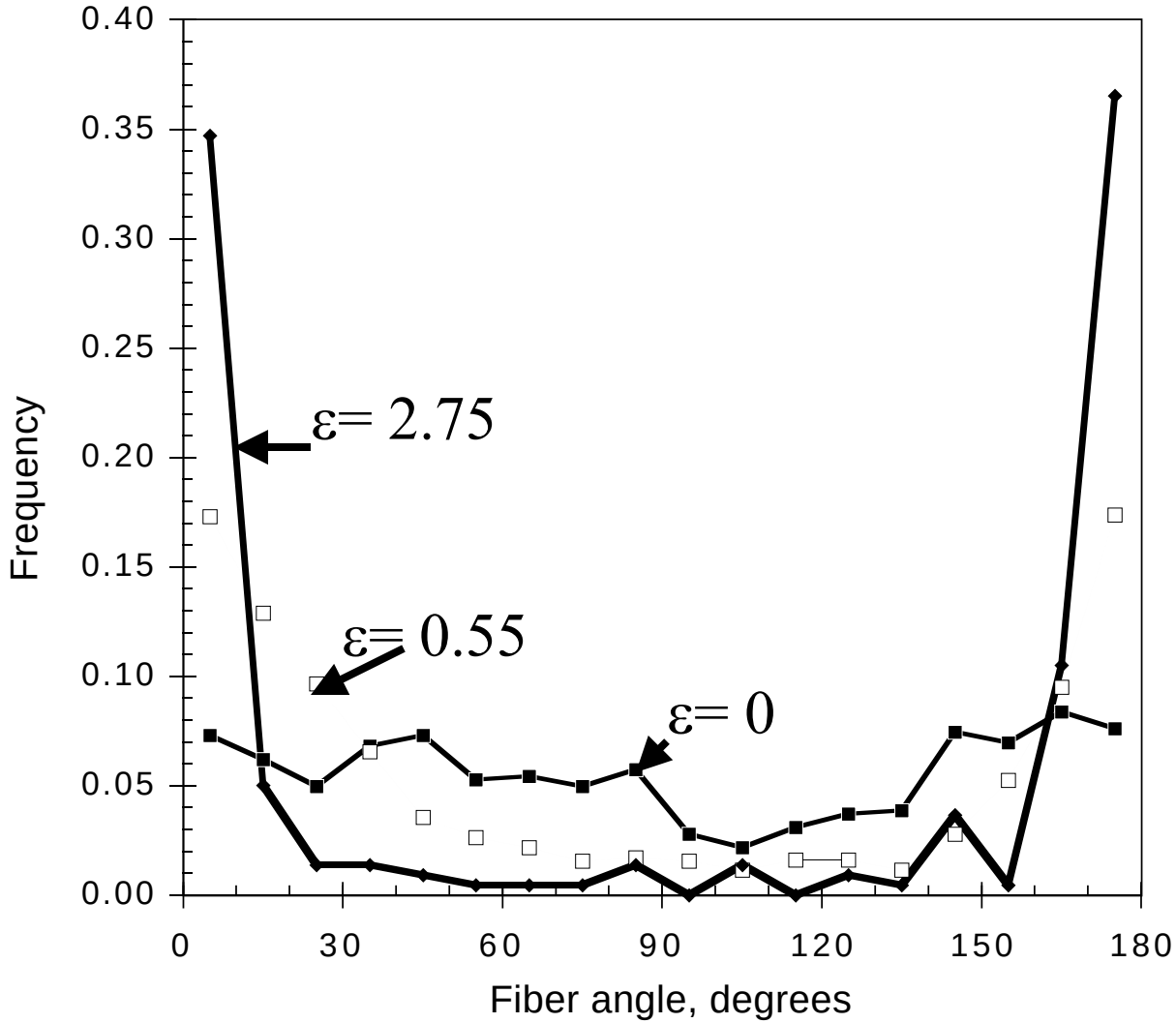

Fiber orientation distributions for strains of 0, 0.55 and 2.75

Figure 37

Why is the rheological characterization of highly filled materials such a challenge?

Wall slip Dependence on the surface/volume ratio
Viscoplasticity Dilatancy
Role of air
Binder migration
Particle migration in the transverse to flow direction

Special tools are necessary plus modified utilization of Conventional rheometers

Figure 38

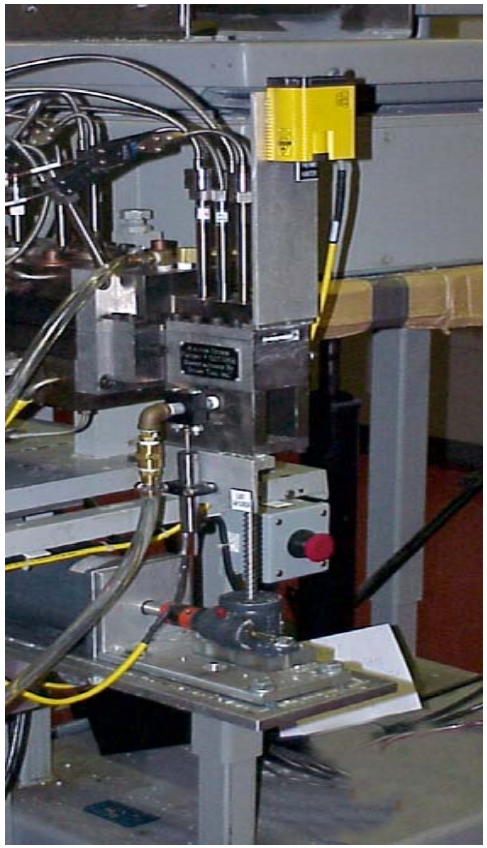

In-house developed Rheometers:

1. **In-line adjustable-gap slit**
   US patent #5,277,058
2. **Off-line adjustable gap slit**
   US patent #5,277,058
3. **Squeeze flow rheometer**

Figure 39

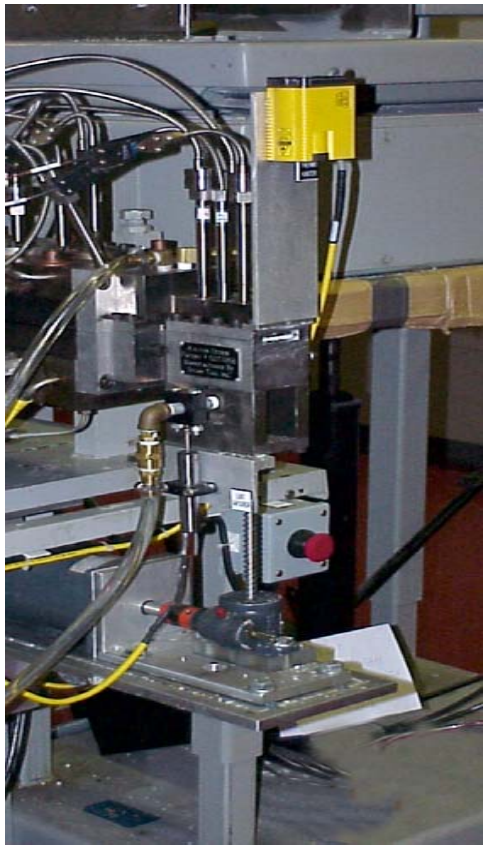

In-line Adjustable Gap Rheometer

- Designed for wall slip and shear viscosity versus shear stress characterization of complex fluids
- Adjustable gap allows the shear rate to be changed at constant flow rate

Figure 40

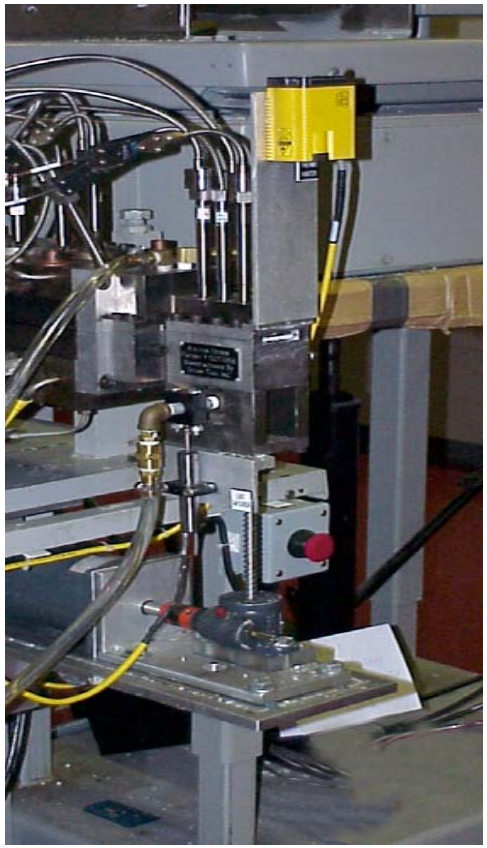

In-line Adjustable Gap Rheometer

Rheometer is connected to single or twin screw extruder and consists of:

- **Rectangular slit die with four pressure transducers,**
- **Facility to change the gap**
- **Computerized data acquisition and analysis**
- **Jacketed for temperature control**

Figure 41

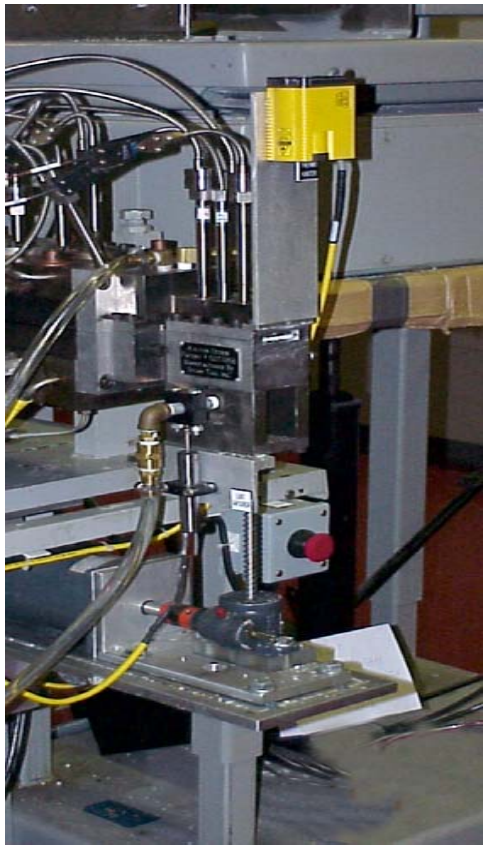

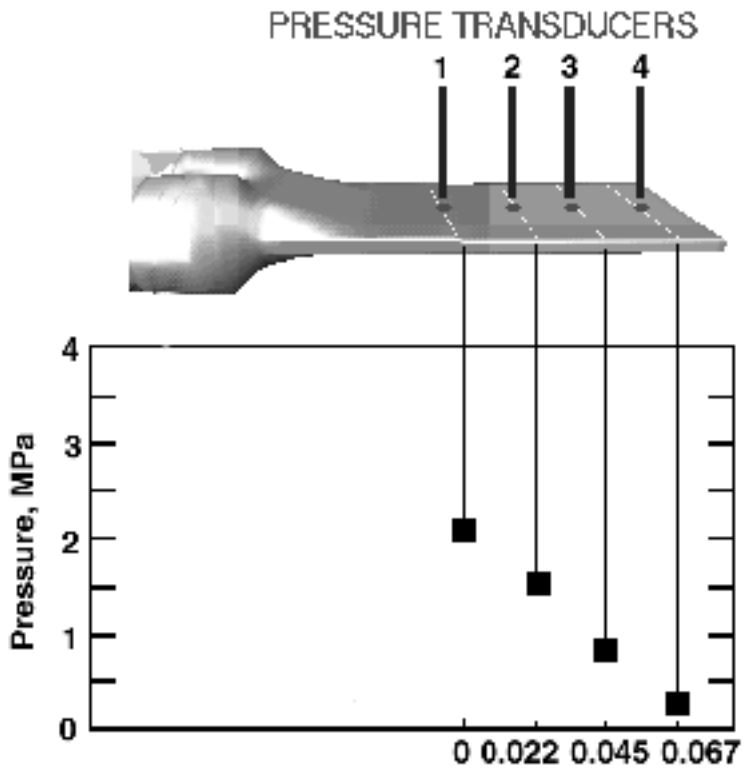

Pressure versus distance in the die

Figure 42

Off-line adjustable gap slit rheometer and fill station

- Allows the complex fluid to be loaded into sealed (if necessary) disposable containers
- Allows vacuum to be applied during the filling (air effect is eliminated)
- Allows the complex fluid to be brought up to the necessary temperature with no exposure to air
- The rheometer is amenable to full automation and is based on the SIT patented adjustable gap concept which facilitates accurate characterization at minimum number of runs

The contents of this file is the proprietary Information of Stevens Institute of Technology

Figure 43

Components of New SIT Rheometry Facility

- Disposable cartridges
- Fill station to fill the cartridges under vacuum
- Integration into an adjustable gap slit rheometer
- Rheometer fits into existing constant crosshead speed Universal Testers

Figure 44

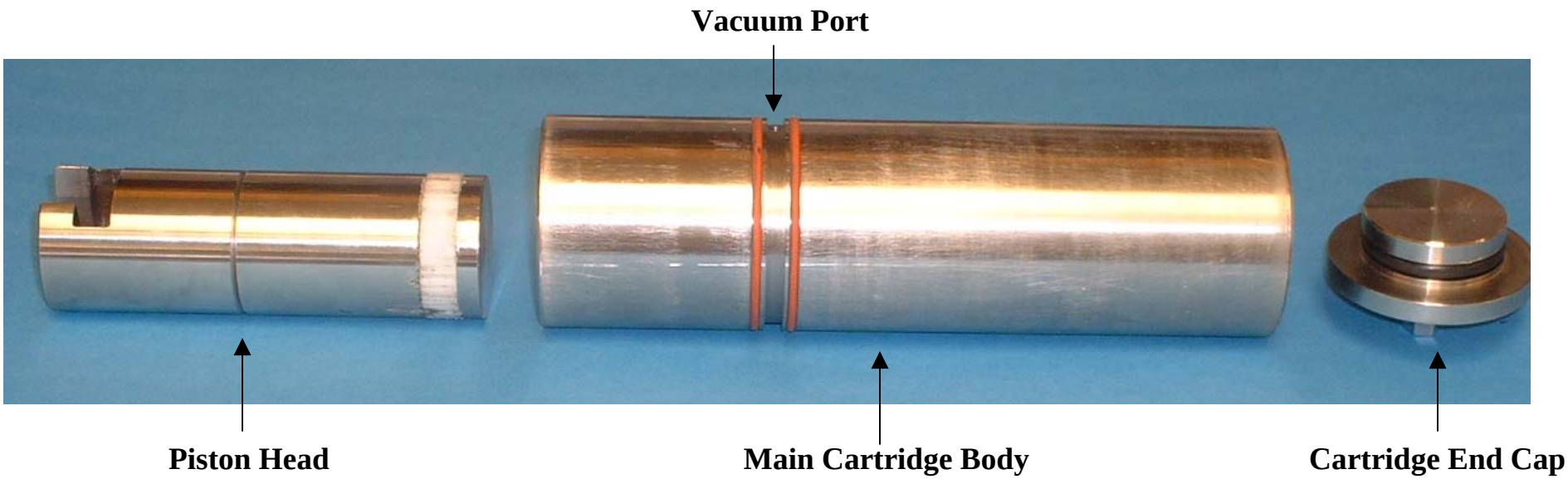

The cartridge assembly is made up of three parts: main body, end cap and piston head. The energetic material is filled into the cartridge assembly under vacuum in the fill station, then conditioned to the desired temperature in a constant temperature oven/environment and then extruded through the rectangular slit die using a ram extruder (Instron Universal Testing Device in our case).

The first step is the preparation of the material for conditioning. The end cap is placed at the bottom of the main cartridge and the nut of the end cap is tightened, which will squeeze and expand the o-ring forming a seal at the bottom of the cartridge. Then the cartridge is pushed into the circulation block of the fill station.

Figure 45

Bi-directional Hydraulic Cylinder that enables movement in horizontal direction

Piston Head

Collar that holds the cartridge in place as the piston moves vertically

Cartridge is inserted into the circulation block

Vacuum Port on fill station

Hand Pump

Circulation Block in which the cartridge assembly sits in

Figure 46

(1) Place some material into the cartridge

(2) Bring the piston head down by the hand pump and compact the material. If necessary raise the piston head up by the reverse action pump and go to step (1) until enough material is compacted into the cartridge under vacuum

Figure 47

Rotate the slit die, circulation block and cartridge assembly upside down so that the slit die faces down

Figure 48

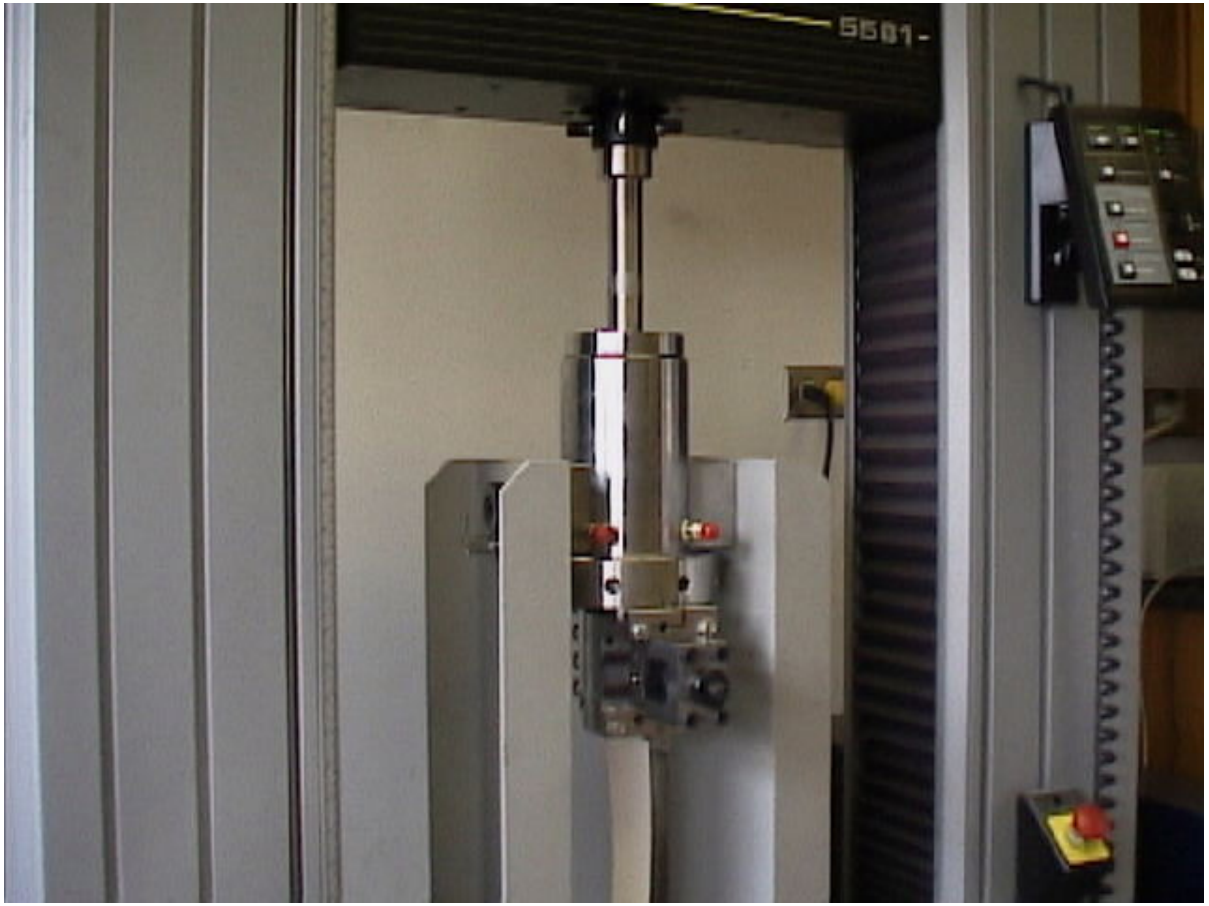

Place the assembly into the Instron tester for the determination
Of the shear stress versus the shear rate behavior of the energetic
Material using a slit rheometer with multiple pressure transducers

Figure 49

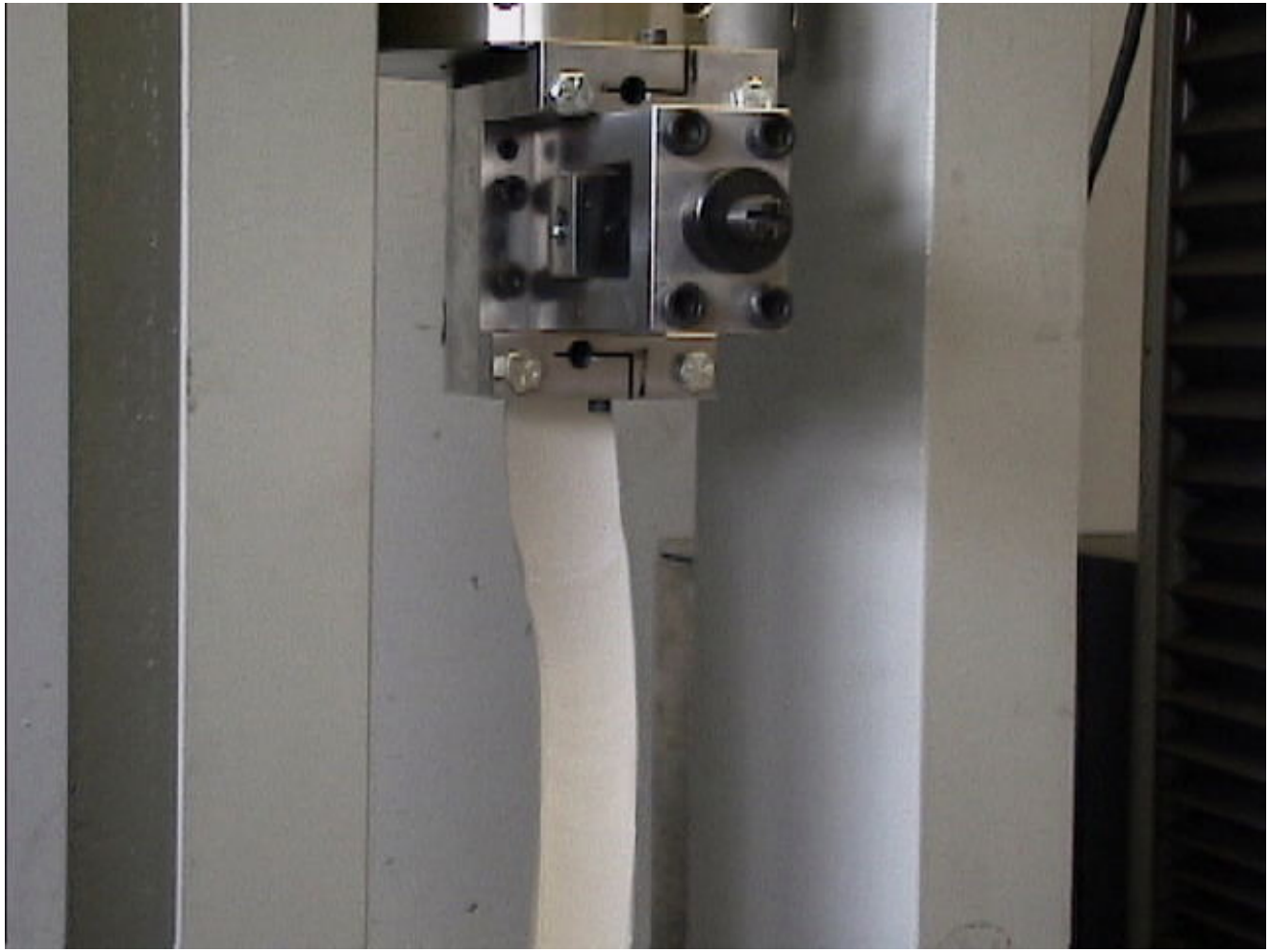

Here we see the extrusion of a strand of a simulant formulation with the rheometer during the characterization of its shear viscosity and wall slip behavior.

Figure 50

Squeeze flow rheometer

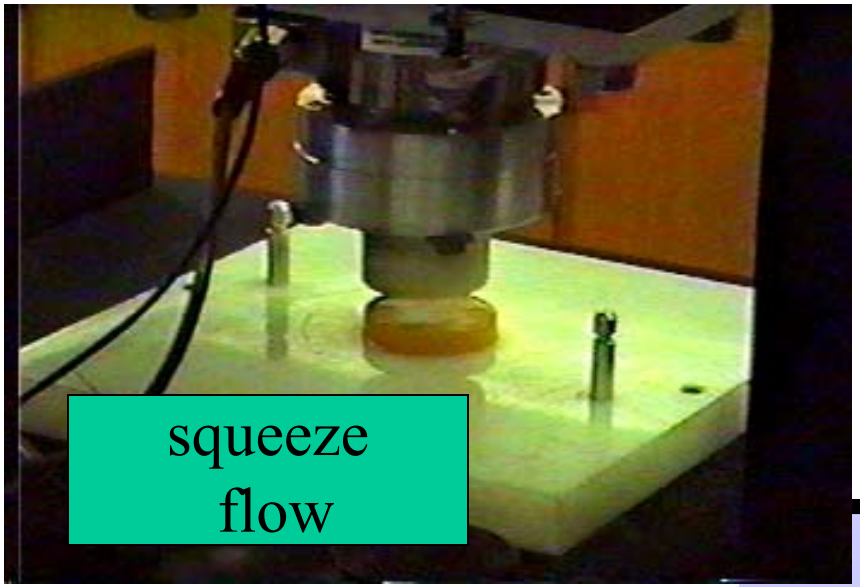

- Simple to operate
- Data analysis instantaneous
- Ideal for complex fluids
- Replaces the “finger” rheometer

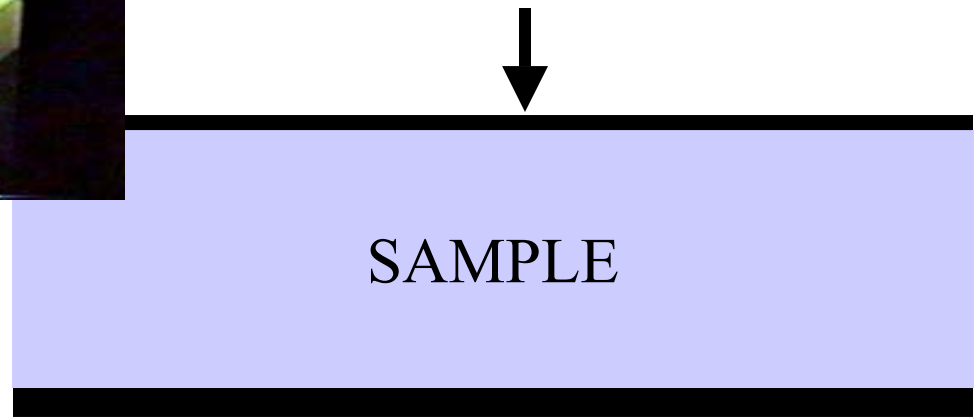

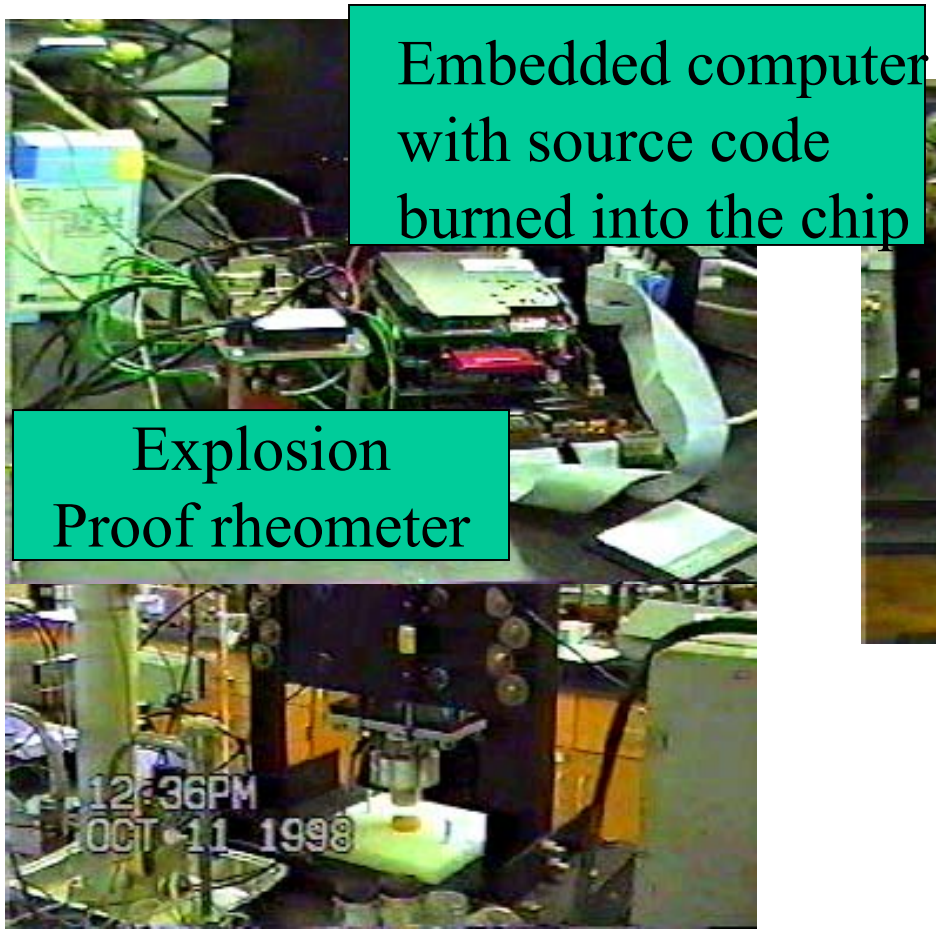

Squeeze flow rheometer

Figure 52

Compressive Squeeze Flow

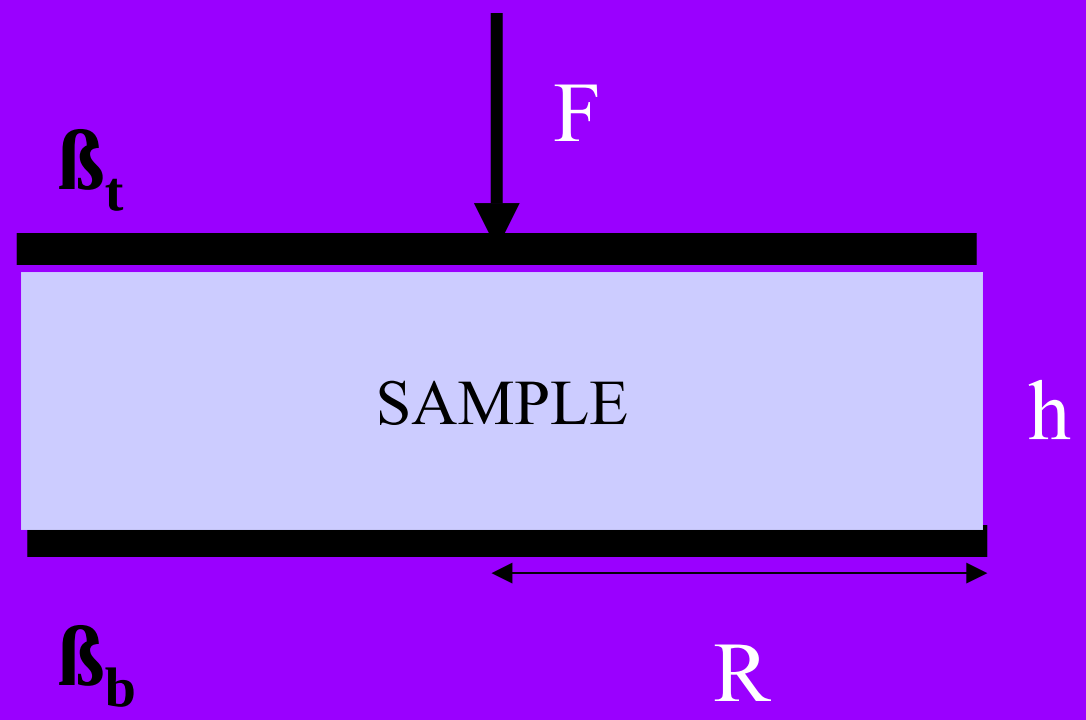

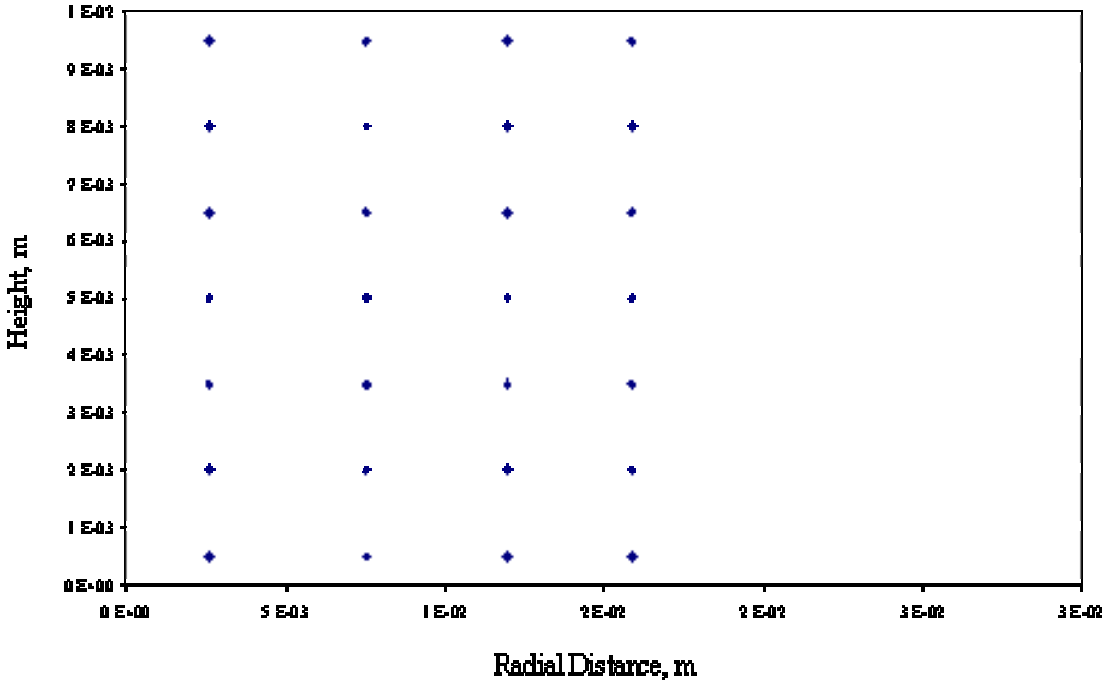
Height, m
Radial Distance, m

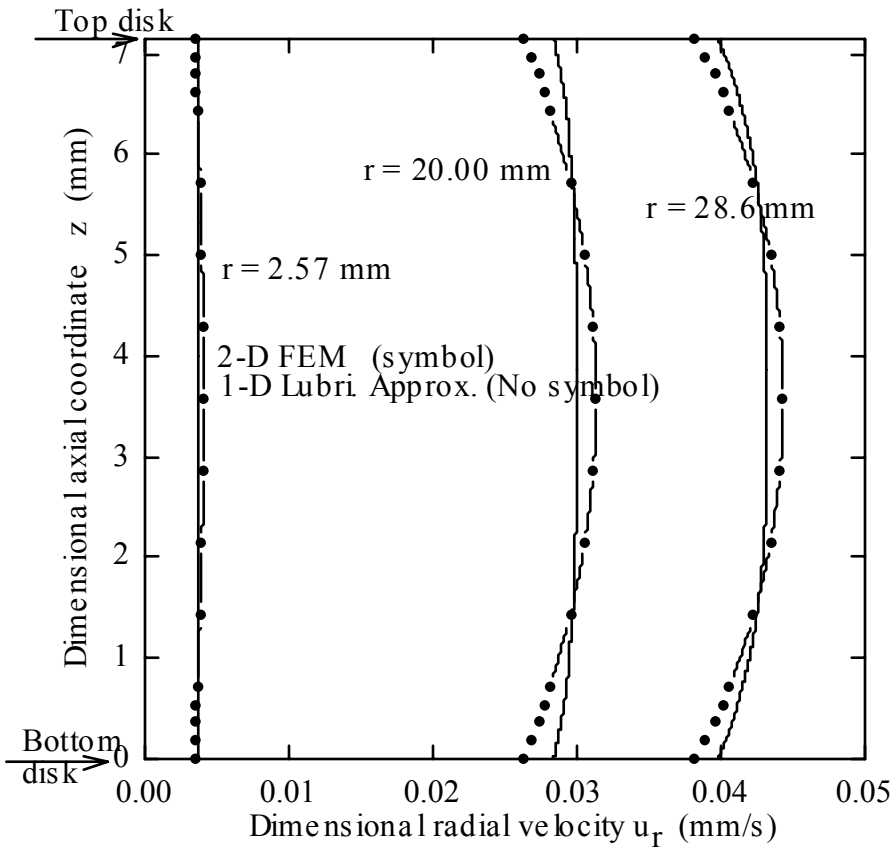

Radial velocity predicted by the 1-D and 2-D analyses of a power law fluid with wall slip; n=0.45, ß*=1.0, h/R=0.25

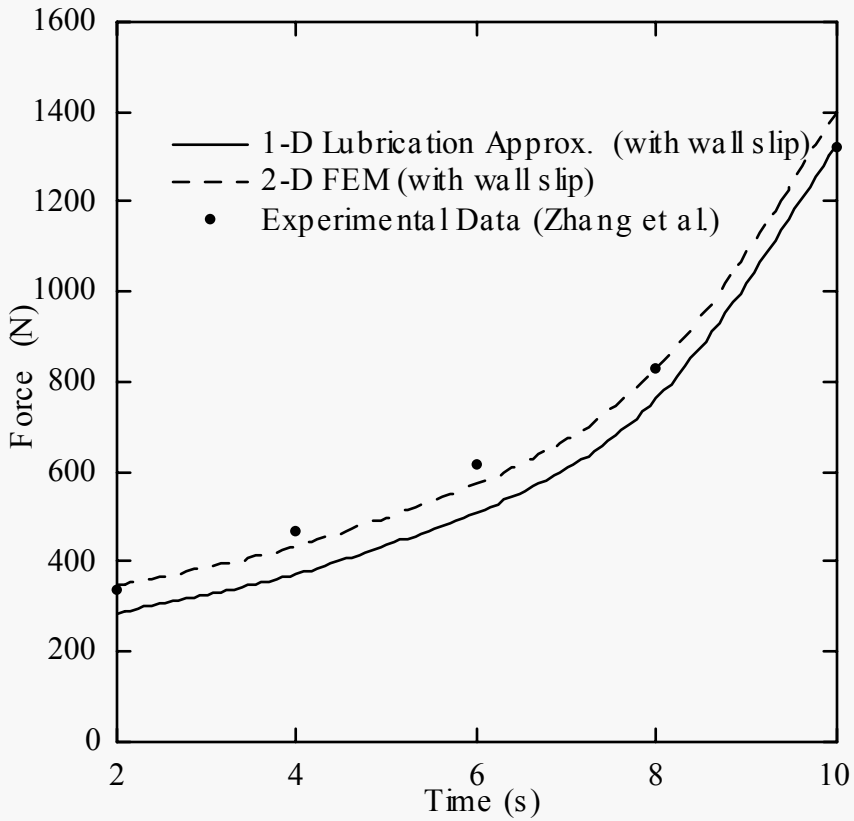

HDPE DuPont 2005, Zhang et al. 1995 data, m=44,900 Pa-s $^{0.25}$, n=0.25, ß=5.13E-15m/(Pa $^{2.35}$ s)

Figure 56

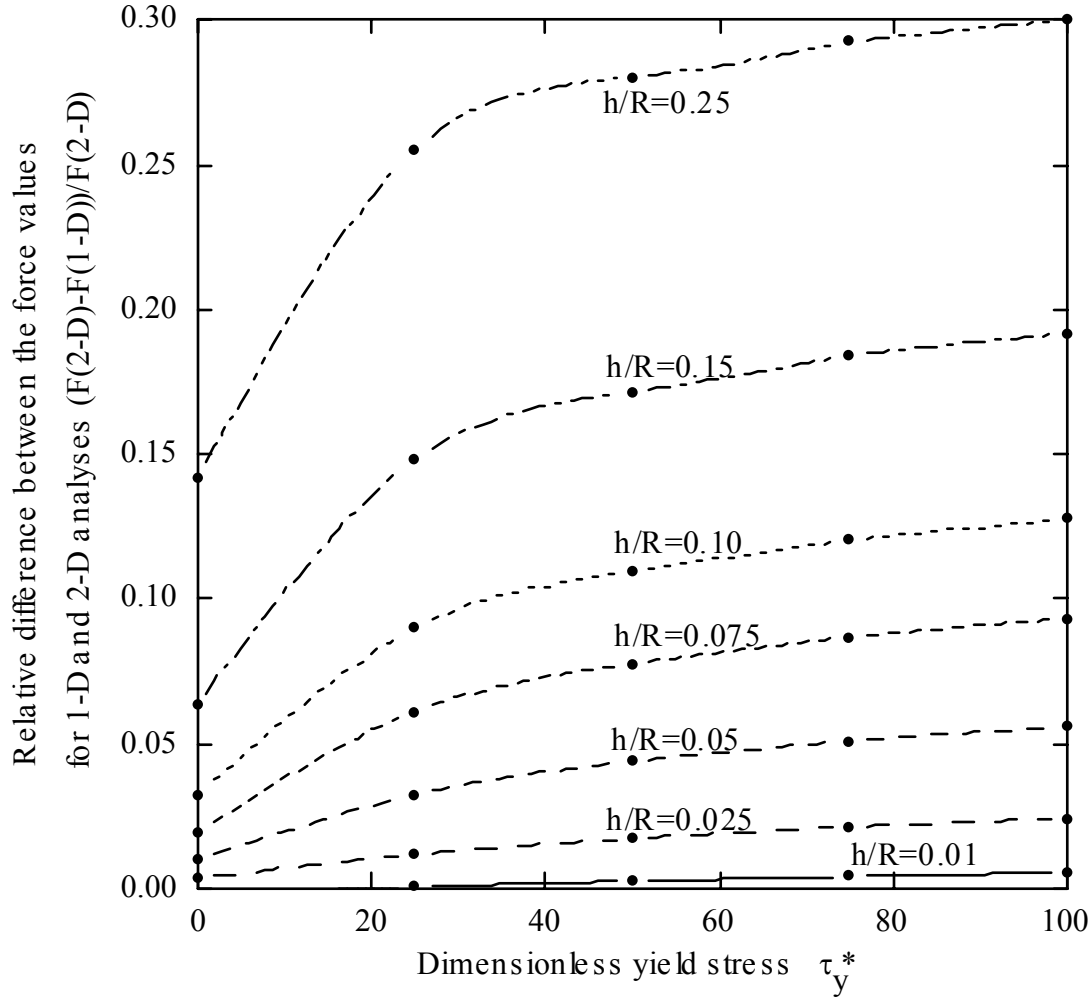

Force values for the 1-D and 2-D analyses vs. yield stress for Herschel-Bulkley fluids with n=0.45 without wall slip.

Highly filled nature of the energetic suspensions

- Give rise to viscoplasticity (solid like behavior in some flow regimes
- Wall slip
- All types of migration effects
- Texturing and flow induced orientation
- These all necessitate novel rheological characterization tools
- Such tools include adjustable-gap slit dies and squeeze flow devices.

Figure 58